This is the peer-reviewed, final accepted version for American Mineralogist, published by the Mineralogical Society of America.
The published version is subject to change. Cite as Authors (Year) Title. American Mineralogist, in press.
DOI: https://doi.org/10.2138/am-2022-8712. http://www.minsocam.org/

Revision 2

Apatite in brachinites: Insights into thermal history and halogen evolution

LANG ZHANG[1], AI-CHENG ZHANG[1,2,*], AND SHU-ZHOU WANG[1]

[a] State Key Laboratory for Mineral Deposits Research, School of Earth Sciences and Engineering, Nanjing University, Nanjing 210023, China

[b] CAS Center for Excellence in Comparative Planetology, China

* E-mail: aczhang@nju.edu.cn

ABSTRACT

Apatite is an important petrogenetic indicator in extraterrestrial materials. Here, we report the mineralogical features of apatite and associated phases in three brachinites Northwest Africa (NWA) 4969, NWA 10637, and NWA 11756. Two types of apatite are observed: intergranular apatite and apatite inclusion within chromite and silicate minerals. The intergranular chlorapatite is enclosed by or penetrated by irregular porous merrillite, indicating chlorapatite replacement by merrillite. The intergranular chlorapatite is closely associated with a fine-grained pyroxene-troilite intergrowth along olivine grain boundaries, which is a sulfidization product of olivine. High-Ca pyroxene is observed as a constituent phase in the intergrowth for the first time. The apatite inclusions are either monomineralic or closely associated with subhedral-euhedral pore-free merrillite. In NWA 4969, the

Always consult and cite the final, published document. See http:/www.minsocam.org or GeoscienceWorld

This is the peer-reviewed, final accepted version for American Mineralogist, published by the Mineralogical Society of America.
The published version is subject to change. Cite as Authors (Year) Title. American Mineralogist, in press.
DOI: https://doi.org/10.2138/am-2022-8712. http://www.minsocam.org/

apatite inclusions show a large compositional variation from chlorapatite to fluorapatite and are systematically more F-rich than intergranular apatite; while the apatite inclusions in NWA 10637 and NWA 11756 are chlorapatite. Most of the two apatite types in brachinites contain oriented tiny or acicular chromite grains, suggesting the exsolution of chromite from apatite. We propose that apatite replacement by merrillite, formation of pyroxene-troilite intergrowth, and exsolution of chromite in apatite were caused by a shock-induced, transient heating event (approximately 930–1000 °C) on the brachinite parent body. This heating event resulted in halogen devolatilization during replacement of the intergranular apatite by merrillite, which probably disturbed the Mn-Cr isotopic system in brachinites as well. We also propose that the apatite inclusions could be a residual precursor material of the brachinites.

Keywords: Apatite, merrillite, halogen, replacement, sulfidization, exsolution, brachinite

INTRODUCTION

Apatite [$Ca_5(PO_4)_3(F,Cl,OH)$] is a ubiquitous mineral in most terrestrial and extraterrestrial materials. It is an important carrier of both volatile elements (F, Cl, and OH) and rare earth elements (REE) (Harlov, 2015; Hughes and Rakovan, 2015). In the past decades, apatite in extraterrestrial materials has been extensively studied to (1) constrain

Always consult and cite the final, published document. See http:/www.minsocam.org or GeoscienceWorld

This is the peer-reviewed, final accepted version for American Mineralogist, published by the Mineralogical Society of America.
The published version is subject to change. Cite as Authors (Year) Title. American Mineralogist, in press.
DOI: https://doi.org/10.2138/am-2022-8712. http://www.minsocam.org/

the petrogenesis and chemical evolution of host rocks (e.g., Shearer et al., 2011; Ward et al., 2017; and references therein); (2) reconstruct the abundance, origin, and evolution of halogen elements and hydrogen on Mars, Moon, and asteroids (e.g., McCubbin and Jones, 2015; McCubbin et al., 2015; Ward et al., 2017; Brearley and Jones, 2018; McCubbin et al., 2021; and references therein); and (3) determine the age of geological events that its host rocks experienced (e.g., Norman and Nemchin, 2014; Yin et al., 2014; Zhang et al., 2016; Zhou et al., 2018; Hu et al., 2019; Li et al., 2021; and references therein).

Brachinites are a group of primitive achondrites that are characterized by the dominance of equigranular FeO-rich olivine (>70 vol%; Krot et al., 2014; Keil, 2014; Mittlefehldt, 2014). Previous investigations have proposed that brachinites are partial melt residues (e.g., Nehru et al., 1983; Day et al., 2012, 2019; Gardner-Vandy et al., 2013; Keil, 2014; Collinet and Grove, 2020; and references therein), although some brachinites have been described as cumulates (Warren and Kallemeyn, 1989; Swindle et al., 1998; Mittlefehldt et al., 2003). Apatite has occasionally been reported in brachinites or some brachinite-like achondrites; however, its mineralogical features and origins have not yet been studied in detail (e.g., Rumble et al., 2008; Hyde et al., 2014; Keil, 2014; Goodrich et al., 2017; Crossley et al., 2020; Ito et al., 2022). All apatite grains reported from brachinites up to date have been chlorapatite (Hyde et al., 2014; Keil, 2014; Goodrich et al., 2017; Crossley et al., 2020; references therein). Hyde et al. (2014) reported that many chlorapatite grains in brachinite Northwest Africa (NWA) 4872 are surrounded by merrillite

Always consult and cite the final, published document. See http:/www.minsocam.org or GeoscienceWorld

This is the peer-reviewed, final accepted version for American Mineralogist, published by the Mineralogical Society of America.
The published version is subject to change. Cite as Authors (Year) Title. American Mineralogist, in press.
DOI: https://doi.org/10.2138/am-2022-8712. http://www.minsocam.org/

61 [$Ca_{18}Na_2Mg_2(PO_4)_{14}$], another common Ca-phosphate mineral in extraterrestrial materials
62 (Jolliff et al., 2006; Shearer et al., 2015). However, the chlorapatite in NWA 4872 was
63 interpreted as an interaction product between merrillite and a Cl-rich melt residuum or low-
64 temperature fluid on the parent body (Hyde et al., 2014).

65 Previous investigations of brachinites focused mainly on their petrogenesis (e.g., Day
66 et al., 2012, 2019; Keil, 2014; Krot et al., 2014; Mittlefehldt, 2014; and references therein).
67 In contrast, their post-formation thermal history, which is an important part of the complete
68 evolutionary history in the parent body of brachinites, was less constrained. Two aspects
69 of petrologic records, that could be related to post-formation heating events, have been
70 reported. First, a few brachinites contain pyroxene-troilite intergrowths (e.g., Rumble et al.,
71 2008; Goodrich et al., 2011, 2017; Singerling et al., 2013; Day et al., 2019), whose
72 formation was recently attributed to a reaction between olivine and a S-rich vapor during
73 an impact-induced heating event (Goodrich et al., 2017). Second, Hyde et al. (2014)
74 proposed an alteration event based on the presence of apatite-merrillite intergrowth in
75 brachinite NWA 4872. However, whether the two events are related to each other remains
76 unknown. In addition, a few geochronological investigations on brachinites indicated that
77 the parent body of the brachinites has a rather complex thermal history (Swindle et al.,
78 1998; Wadhwa et al., 1998; Mittlefehldt et al., 2003; Beard et al., 2016; Dunlap et al.,
79 2016a,b). For instance, brachinites have large variations in Mn-Cr and Ar-Ar ages from
80 4564.8 Ma to ~200 Ma, with some of the ages being attributed to impact events (Dunlap et

Always consult and cite the final, published document. See http:/www.minsocam.org or GeoscienceWorld

This is the peer-reviewed, final accepted version for American Mineralogist, published by the Mineralogical Society of America.
The published version is subject to change. Cite as Authors (Year) Title. American Mineralogist, in press.
DOI: https://doi.org/10.2138/am-2022-8712. http://www.minsocam.org/

al., 2016a). However, most of these ages were not discussed in the context of petrologic observations of the brachinites. Recently, Ito et al. (2022) reported young U-Pb ages (<4.5 Ga) of apatite and merrillite in the brachinite NWA 10932 and suggested that an internal heat source rather than impact may be responsible for the formation of phosphate.

To further constrain the thermal history of brachinites, we have performed comprehensive petrographic and mineralogical investigations on three brachinites (NWA 4969, NWA 10637, and NWA 11756). This paper reports the petrography and mineral compositions of apatite and associated minerals in the three brachinites and we then discuss their significance with respect to the thermal history and halogen evolution in the parent body of the brachinites. Preliminary results have been reported in two abstracts in Chinese (Zhang et al., 2021a, 2021b).

SAMPLES AND ANALYTICAL METHODS

NWA 4969, NWA 10637, and NWA 11756 were classified as brachinites in Meteoritical Bulletin Database (c.f., Connolly et al., 2008; Bouvier et al., 2017; Gattacceca et al., 2020). The petrography and mineralogy of NWA 4969 and NWA 11756 have been briefly reported in conference abstracts or journal articles (e.g., Rumble et al., 2008; Gardner-Vandy et al., 2013; Crossley et al., 2020); however, the petrography and mineralogy of NWA 10637 has only been reported in Meteoritical Bulletin Database (Bouvier et al., 2017). The oxygen isotope composition of NWA 10637 ($\Delta^{17}O$ = –0.263 to

Always consult and cite the final, published document. See http:/www.minsocam.org or GeoscienceWorld

This is the peer-reviewed, final accepted version for American Mineralogist, published by the Mineralogical Society of America.
The published version is subject to change. Cite as Authors (Year) Title. American Mineralogist, in press.
DOI: https://doi.org/10.2138/am-2022-8712. http://www.minsocam.org/

101 –0.126 ‰) was also reported in the Database, helping to confirm NWA 10637 is a
102 brachinite (Bouvier et al., 2017). The three brachinite samples in the present study were
103 purchased from meteorite dealers.

104 Petrographic observations of the three samples were carried out with the Zeiss Supra
105 55 field emission scanning electron microscope (FE-SEM) at Nanjing University, Nanjing,
106 China. The FE-SEM instrument was operated at a 15-kV accelerating voltage. Energy
107 dispersive spectroscopic (EDS) point analyses and elemental mapping were also used to
108 qualitatively identify minerals in the regions of interest. Mosaic backscattered electron
109 (BSE) imaging and X-ray elemental mapping for the polished sections were carried out
110 and used for calculating the modal abundances of the constituent minerals.

111 Mineral compositions were measured using the JEOL 8100 and 8230 electron probe
112 micro-analyzers (EPMA) at Nanjing University. A 20-nA beam accelerated at 15 kV was
113 used for the EPMA analyses of silicate and oxide minerals. However, a 10-nA beam
114 accelerated at 10 kV was used for the measurements of merrillite. Olivine, pyroxene,
115 chromite, and merrillite were analyzed with a focused beam; whereas plagioclase was
116 analyzed with a defocused beam (3 μm). For most elements, the counting times for the
117 peak and background measurements were 20 s and 10 s, respectively. However, 10 s and
118 5 s were used for peak and background measurements of Na and K, respectively. Sodium
119 and K were the first elements measured on their respective spectrometer crystals. Natural
120 fayalite for Fe and Mn, forsterite for Mg, hornblende for Si, Al, Ca, Ti, Na, K, and Durango

Always consult and cite the final, published document. See http:/www.minsocam.org or GeoscienceWorld

This is the peer-reviewed, final accepted version for American Mineralogist, published by the Mineralogical Society of America.
The published version is subject to change. Cite as Authors (Year) Title. American Mineralogist, in press.
DOI: https://doi.org/10.2138/am-2022-8712. http://www.minsocam.org/

fluorapatite for P and synthetic Cr_2O_3 for Cr were used as standards for concentration calibration.

Quantitative measurements of apatite with EPMA are challenging, especially for some apatite grains in this study that have very low F concentrations. We used the LDE1 crystal for determining the F concentration in apatite. Due to the low concentration of F in most apatite grains in the present study, we performed qualitative scanning on Durango apatite standard and some apatite grains in the present study prior to quantitative measurements at various accelerating voltages (10 kV, 12 kV, and 15 kV), beam currents (5 nA, 10 nA, and 20 nA), and focusing modes (focused and 3 μm defocused). Eventually, an accelerating voltage of 15 kV and a defocused 3 μm beam of 20 nA were settled upon for the apatite analyses, since repeatable results could be obtained with this analytical condition for the standards. The elemental peak for F was preset to an L value (the distance between X-ray source and LDE1 analyzing crystal) of 84.15 mm and the lower and upper backgrounds were preset to −6 mm and +17 mm, respectively, based on qualitative scanning results. Chlorine and F were the first elements measured on their respective spectrometer crystals. Durango fluorapatite was used as the standard for P, Ca, and F. A synthetic $Ba_5(PO_4)_3Cl$ crystal was used as the standard for Cl. Standards for other elements are the same as those for the silicate minerals mentioned above. All the EPMA data was reduced using the ZAF correction procedure. Based on multiple analyses on Durango fluorapatite and $Ba_5(PO_4)_3Cl$, the uncertainties for Cl and F are better than 7%. However,

Always consult and cite the final, published document. See http:/www.minsocam.org or GeoscienceWorld

This is the peer-reviewed, final accepted version for American Mineralogist, published by the Mineralogical Society of America.
The published version is subject to change. Cite as Authors (Year) Title. American Mineralogist, in press.
DOI: https://doi.org/10.2138/am-2022-8712. http://www.minsocam.org/

the potential anisotropic diffusion effect was not considered in the present study (Henderson, 2011 and references therein). Hence, it is possible that the analytical uncertainties for the concentrations of Cl and F might be larger than 7%.

Trace element concentrations in apatite and merrillite were measured using laser ablation-inductively coupled plasma mass spectrometry (LA-ICP-MS) at Nanjing University. The target minerals were ablated using a Reso LR155 Excimer 193 nm laser ablation system, connected to ICap Q mass spectrometer. A 4-Hz laser repetition rate was used for the ablation. A 20-μm laser spot size was used for the analyses. The counting times for both background and target phases are 30 s. Durango was used as the external standard; while other four synthetic glasses NIST-610, NIST-612, and NIST-614 were measured as unknowns to monitor data quality. Calcium was used as the internal standard. Trace element abundances were calculated by normalizing the CaO contents in the apatite and merrillite to the values measured by EPMA. Data reduction was performed using the ICPMSDataCal (V9.5) software package (Liu et al., 2008).

RESULTS

General petrography of the three brachinites

Representative mosaic BSE images and elemental mapping results of the three brachinites are shown in the supplementary figures (Figs. S1–S3). All three brachinites show an equigranular texture of silicate minerals (mainly 300–800 μm in grain size).

Always consult and cite the final, published document. See http:/www.minsocam.org or GeoscienceWorld

This is the peer-reviewed, final accepted version for American Mineralogist, published by the Mineralogical Society of America.
The published version is subject to change. Cite as Authors (Year) Title. American Mineralogist, in press.
DOI: https://doi.org/10.2138/am-2022-8712. http://www.minsocam.org/

Olivine is the dominant phase but has various modal abundances among different samples (94 vol% in NWA 4969; 73 vol% in NWA 10637; 72 vol% in NWA 11756; Table 1). Pyroxene also has a large variation in modal abundance. In NWA 4969, the intergranular pyroxene is high-Ca pyroxene (2.4 vol%); no intergranular orthopyroxene grains were observed. Both NWA 10637 and NWA 11756 have high abundances of pyroxene (20.7 vol% and 19.8 vol%, respectively). The intergranular pyroxene therein contains both orthopyroxene and high-Ca pyroxene, and orthopyroxene is dominant (Table 1). In these brachinites, chromite, plagioclase, Ca-phosphate minerals, and troilite occur as accessory phases with various abundances (Table 1). A few rounded olivine, pyroxene, and Ca-phosphate inclusions (< 100 μm) are also observed (e.g., Fig. S4). Fe-oxide/hydroxide, a terrestrial weathering product of Fe-Ni metal and/or sulfide, is widely observed in all three samples. However, the abundance of Fe-oxide/hydroxide phases in NWA 4969 is much lower than in NWA 10637 and NWA 11756 (Table 1; Figs. S1–S3). An amorphous Fe-phosphate phase, a possible terrestrial weathering product (Hyde et al., 2014), was also observed in NWA 4969 and NWA 11756.

Fine-grained pyroxene-troilite intergrowths, which have been reported in a few other brachinites (e.g., Rumble et al., 2008; Day et al., 2012; Goodrich et al., 2011, 2017), also occur along olivine grain boundaries in all three brachinites in this study (Fig. 1). However, in contrast to previous investigations, our elemental mapping results reveal that the intergrowths contain not only orthopyroxene but also high-Ca pyroxene, although the latter

Always consult and cite the final, published document. See http:/www.minsocam.org or GeoscienceWorld

This is the peer-reviewed, final accepted version for American Mineralogist, published by the Mineralogical Society of America.
The published version is subject to change. Cite as Authors (Year) Title. American Mineralogist, in press.
DOI: https://doi.org/10.2138/am-2022-8712. http://www.minsocam.org/

is less abundant (Fig. 1). Some tiny metal grains (< 1 μm) also occur in a few intergrowths. It is noteworthy that the pyroxene-troilite intergrowth is common in NWA 4969 and NWA 11756. However, in NWA 10637, only four small regions, (< 30 μm in the largest dimension), containing a potential pyroxene-troilite intergrowth, were observed. Here high-Ca pyroxene is very rare (only 3 submicron high-Ca pyroxene grains in three of the four regions).

Mineralogy of apatite and associated merrillite

Apatite has two different occurrences in the three brachinites. One is as intergranular apatite between silicate minerals and is always associated with merrillite (Fig. 2). The other is as rounded apatite included within chromite or silicate minerals (Figs. 3 and 4). Both types of apatite are present in NWA 4969 and NWA 11756; however, in NWA 10637, apatite occurs only as mineral inclusion.

In NWA 4969, intergranular apatite is commonly surrounded by merrillite (Figs. 2a and 2b). The outlines of the apatite-merrillite assemblage conform to the shapes of the surrounding equi-granular silicate grains. The grain boundaries between apatite and merrillite are irregularly shaped (Figs. 2a and 2b). Many intergranular merrillite grains in NWA 4969 contain submicron-sized pores adjacent to the boundary with apatite (Figs. 2a and 2c). The intergranular apatite-merrillite assemblage is spatially associated with pyroxene-troilite intergrowths (Figs. 2a and 2b). In the polished sections made from NWA

Always consult and cite the final, published document. See http:/www.minsocam.org or GeoscienceWorld

This is the peer-reviewed, final accepted version for American Mineralogist, published by the Mineralogical Society of America.
The published version is subject to change. Cite as Authors (Year) Title. American Mineralogist, in press.
DOI: https://doi.org/10.2138/am-2022-8712. http://www.minsocam.org/

4969, about 50 apatite inclusions were observed. Most of them are included in chromite and monomineralic. A few apatite inclusions themselves contain subhedral-euhedral, pore-free merrillite grains at their margins, which is different from the texture of the intergranular apatite and merrillite. An apatite aggregate of approximately 40 μm in size included within one chromite grain shows a marked Z-contrast variation in the BSE image (Fig. 3a). Elemental mapping results demonstrate that the Z-contrast variation among and within the apatite grains is related to variations in the Cl and F contents (Figs. 3c and 3d). High-magnification SEM observations show that both the intergranular apatite and the apatite inclusions usually contain oriented tiny or acicular chromite inclusions (Fig. 2c). In addition, tiny chromite grains (submicron in size) also occur at the grain boundaries between the apatite and adjacent olivine (Fig. 2d).

In NWA 11756, the intergranular chlorapatite-merrillite assemblage also has outlines conforming to the shapes of the surrounding silicate grains (Figs. 2e and 2f). However, the texture of the chlorapatite-merrillite assemblage differs slightly from that in NWA 4969. First, the merrillite/chlorapatite volume ratio in NWA 11756 appears to be lower than that in NWA 4969. Second, merrillite in NWA 11756 mainly appears as irregular grains along fractures in the chlorapatite and along the interface with the surrounding silicate phases. Small pores also occur in a few intergranular merrillite grains in NWA 11756, although less common than in NWA 4969. The intergranular apatite-merrillite assemblage in NWA 11756 is also spatially associated with a pyroxene-troilite intergrowth (Fig. 2e). The apatite

Always consult and cite the final, published document. See http:/www.minsocam.org or GeoscienceWorld

This is the peer-reviewed, final accepted version for American Mineralogist, published by the Mineralogical Society of America.
The published version is subject to change. Cite as Authors (Year) Title. American Mineralogist, in press.
DOI: https://doi.org/10.2138/am-2022-8712. http://www.minsocam.org/

221 inclusions (5–100 μm) in NWA 11756 mainly occur within olivine and orthopyroxene. In
222 one case, the olivine grain containing a subhedral-euhedral apatite grain is itself included
223 within a coarse chromite grain (Fig. 4a). Most apatite inclusions in NWA 11756 are also
224 closely associated with merrillite. Differing from the intergranular merrillite, most of the
225 merrillite grains associated with the apatite inclusions are subhedral to euhedral in shape
226 and included by the latter (Fig. 4b). They are pore-free and sometimes contain tiny sulfide
227 grains. Similar to apatite in NWA 4969, the intergranular apatite grains and the apatite
228 grains in NWA 11756 also contain tiny chromite grains in the grain interiors and some of
229 the chromite grains are acicular (Figs. 2e and 2f). Some tiny chromite grains also occur at
230 the grain boundaries between the apatite inclusions and the host silicate minerals (Fig. 4b).
231 In NWA 10637, the apatite grains are present only as inclusions (Figs. 4c and 4d). No
232 intergranular apatite grains were observed in this study. The apatite inclusions usually form
233 intergrowths (10–30 μm) with subhedral-euhedral merrillite. In some cases, euhedral
234 merrillite grains are totally included in apatite (Fig. 4c). Tiny chromite grains (<1 μm) are
235 commonly observed at the boundaries between included apatite and the host olivine (Figs.
236 4c and 4d).
237
238 **Major- and minor-element compositions of minerals**

Always consult and cite the final, published document. See http:/www.minsocam.org or GeoscienceWorld

This is the peer-reviewed, final accepted version for American Mineralogist, published by the Mineralogical Society of America.
The published version is subject to change. Cite as Authors (Year) Title. American Mineralogist, in press.
DOI: https://doi.org/10.2138/am-2022-8712. http://www.minsocam.org/

239 EPMA compositions of the major and minor elements in minerals from the three
240 brachinites (olivine, pyroxene, plagioclase, chromite, and Ca-phosphates) are reported in
241 the supplementary Tables S1 through S7.

242 All olivine grains in the three brachinites are FeO-rich. The Fo values
243 (≡100*Mg/(Mg+Fe)) of equi-granular olivine in NWA 4969, NWA 10637, and NWA 11756
244 are 65.4–66.4, 72.7–73.7, and 72.7–73.8, respectively. The olivine inclusions in NWA 4969
245 are more magnesian ($Fo_{66.7–68.2}$) than the equi-granular olivine in the same sample; while
246 the compositions of the olivine inclusions in NWA 10637 and NWA 11756 are comparable
247 to those of the intergranular olivine grains in the same samples (Table S1).

248 Major-element and minor-element compositions of pyroxenes in the three brachinites
249 are illustrated in Figs. 5–7. The intergranular high-Ca pyroxene in NWA 4969 contains
250 slightly higher Wo components than those in NWA 10637 and NWA 11756 (Table S2; Fig.
251 5a). The Al_2O_3, TiO_2, and Cr_2O_3 contents are comparable among the intergranular high-Ca
252 pyroxene in the three brachinites (Fig. 6). Intergranular orthopyroxene grains in NWA
253 10637 and NWA 11756 have essentially identical major-element compositions (Table S2;
254 Fig. 5). They have similar TiO_2 and Cr_2O_3 contents and slightly different Al_2O_3 contents
255 (Table S2; Fig. 7). Based on the two-pyroxene thermometer in Brey and Kohler (1990),
256 paired high-Ca pyroxene and orthopyroxene give an equilibrium temperature of 929 ±
257 21 °C and 972 ± 10 °C for NWA 10637 and NWA 11756, respectively. Compositions of
258 the orthopyroxene inclusions within chromite from NWA 10637 and NWA 11756 were

Always consult and cite the final, published document. See http:/www.minsocam.org or GeoscienceWorld

This is the peer-reviewed, final accepted version for American Mineralogist, published by the Mineralogical Society of America.
The published version is subject to change. Cite as Authors (Year) Title. American Mineralogist, in press.
DOI: https://doi.org/10.2138/am-2022-8712. http://www.minsocam.org/

also measured. However, the data show anomalously high Cr_2O_3 contents (1.4–1.7 wt%), which could be due to potential analytical contamination from the host chromite. Therefore, the data are not reported here.

Fine-grained high-Ca pyroxene and orthopyroxene in the pyroxene-troilite intergrowths from NWA 10637 have major-element compositions essentially identical to those from NWA 11756 (Table S3; Fig. 5), respectively. However, high-Ca pyroxene and orthopyroxene in the intergrowths from NWA 4969 have major-element compositions different from those in NWA 10637 and NWA 11756 (Table S3; Fig. 5). The high-Ca pyroxene and orthopyroxene in the intergrowths show systematically lower contents of Al_2O_3, TiO_2, and Cr_2O_3 than those in the intergranular pyroxenes from the same samples (Table S3; Figs. 6 and 7). Based on the two-pyroxene thermometer in Brey and Kohler (1990), the paired high-Ca pyroxene and orthopyroxene in the intergrowths give an equilibrium temperature of 1015 ± 16 °C, 932 ± 63 °C, and 938 ± 51 °C for NWA 4969, NWA 10637, and 11756, respectively.

Plagioclase grains in both NWA 10637 and NWA 11756 are mainly sodic and have similar An values (An=34.6–35.4 and 33.1–35.1, respectively; Table S4). Only the coarse chromite grains in the three brachinites were measured. The chromite grains in NWA 10637 and NWA 11756 have essentially identical compositions. They have higher Cr# (≡100*Cr/(Al+Cr)) values (77.1–77.7) than those in NWA 4969 (73.0–73.5; Table S5).

Always consult and cite the final, published document. See http:/www.minsocam.org or GeoscienceWorld

This is the peer-reviewed, final accepted version for American Mineralogist, published by the Mineralogical Society of America.
The published version is subject to change. Cite as Authors (Year) Title. American Mineralogist, in press.
DOI: https://doi.org/10.2138/am-2022-8712. http://www.minsocam.org/

Their TiO_2 contents (1.0–1.1 wt%) are also higher than those in chromite from NWA 4969 (0.56–0.64 wt%).

The F-Cl compositions from apatite are plotted in a ternary diagram for F, Cl, and the missing component, likely OH (Fig. 8). The amounts of the missing component are assumed to be 1–F–Cl. The present study mainly focuses on the fluorapatite and chlorapatite components. The intergranular apatite grains in NWA 4969 are chlorapatite with a 10 to 16 mol% fluorapatite component (Table S6; Fig. 8a). Most of the apatite inclusions in NWA 4969 are also chlorapatite, but contain a fluorapatite component comparable to or higher than those of the intergranular grains (Table S6; Fig. 8a). A few apatite inclusions (Fig. 3) are fluorapatite with fluorapatite component high up to 78 mol%. The fluorapatite grains contain much lower Na_2O (< 0.06 wt%) than the chlorapatite (0.3–0.6 wt%). The apatite inclusions in NWA 10637 are also chlorapatite, with the fluorapatite component varying from 0 to 13 mol% (Fig. 8b). The intergranular apatite grains and the apatite inclusions in NWA 11756 have comparable compositions with the fluorapatite component varying from 4 mol% to 18 mol% (Fig. 8c). The chlorapatite in NWA 10637 and NWA 11756 contains a similar Na_2O content (0.3–0.5 wt%).

The merrillite grains in this study have similar MgO contents (Table S7). There are small variations in FeO and Na_2O between different samples or between different occurrences (Table S7). The merrillite grains associated with intergranular apatite and apatite inclusions in NWA 4969 have similar FeO (0.83–1.21 wt% and 0.88–1.28 wt%,

Always consult and cite the final, published document. See http:/www.minsocam.org or GeoscienceWorld

This is the peer-reviewed, final accepted version for American Mineralogist, published by the Mineralogical Society of America.
The published version is subject to change. Cite as Authors (Year) Title. American Mineralogist, in press.
DOI: https://doi.org/10.2138/am-2022-8712. http://www.minsocam.org/

298 respectively) and Na_2O (2.62–2.96 wt% and 2.68–2.92 wt%, respectively) contents. The
299 FeO contents in the intergranular merrillite from NWA 11756 (0.52–1.02 wt%) are
300 comparable to those in NWA 4969. However, the merrillite inclusions in NWA 10637 and
301 NWA 11756 have FeO contents (1.15–1.45 wt% and 1.35–1.64 wt%) slightly higher than
302 those in NWA 4969. The merrillite grains associated with intergranular apatite and apatite
303 inclusions in NWA 10637 and NWA 11756 show similar Na_2O contents (1.75–2.64 wt%),
304 which are slightly lower than those in NWA 4969.
305
306 **Trace-element concentrations of intergranular apatite and merrillite**
307 In total, 21 trace-element point analyses were carried out on intergranular apatite and
308 associated merrillite. The data are given in Tables S8 and illustrated in Figs. 9 and 10. Both
309 intergranular apatite and merrillite in NWA 4969 exhibit a generally flat REE pattern with
310 a small positive Eu anomaly (Eu/Eu* = 1.3–3.8, where Eu/Eu* $\equiv$ $Eu_N/\sqrt{(Sm_N*Gd_N)}$; Fig.
311 9a). The REE concentrations in merrillite (La=17.5–22.2*CI) from NWA 4969 are
312 approximately two times higher than those of chlorapatite (La=6.6–10.4*CI; Table S8).
313 The apatite and merrillite in NWA 11756 also show flat REE patterns with a small positive
314 Eu anomaly (1.6–11.6; Fig. 9b). However, the merrillite REE concentration (La=16.6*CI)
315 is much higher than that of apatite (1.0–3.7*CI; Table S8; Fig. 9b).

Always consult and cite the final, published document. See http:/www.minsocam.org or GeoscienceWorld

This is the peer-reviewed, final accepted version for American Mineralogist, published by the Mineralogical Society of America.
The published version is subject to change. Cite as Authors (Year) Title. American Mineralogist, in press.
DOI: https://doi.org/10.2138/am-2022-8712. http://www.minsocam.org/

316 Both the apatite and merrillite grains in this study have low concentrations of Th
317 (0.15–0.34 ppm and 0.18–0.37 ppm, respectively) and U (0.02–0.15 ppm and 0.02–0.19
318 ppm, respectively; Fig. 10). No sample- or mineral-dependent variations were observed.
319

320 # DISCUSSION

321 ## Replacement of intergranular apatite by merrillite

322 In extraterrestrial materials, apatite and merrillite show various textural relationships
323 (e.g., Zhang et al., 2010; Shearer et al., 2011; Day et al., 2012; Sarafian et al., 2013; Hyde
324 et al., 2014; Jones et al., 2014, 2016; Howarth et al., 2015; McCubbin and Jones, 2015;
325 Zhang et al., 2016; Ward et al., 2017). Apatite and merrillite in lunar and Martian basalts
326 usually occur either as subhedral-euhedral individual grains or show an intergrowth texture
327 (e.g., Zhang et al., 2010; Howarth et al., 2015; McCubbin and Jones, 2015). In lunar
328 samples, this feature was interpreted to be a co-crystallization from basaltic melts (e.g.,
329 Zhang et al., 2010). However, their coexistence in Martian basalts was interpreted as a
330 reaction product between merrillite and a Cl-rich hydrothermal fluid (e.g., Howarth et al.,
331 2015; McCubbin and Jones, 2015; McCubbin et al., 2016). Jones et al. (2014) and
332 McCubbin and Jones (2015) proposed that the chlorapatite in chondritic meteorites formed
333 through reactions between merrillite and metasomatic fluids. A similar interpretation has
334 also been applied to the complex textural relationship between chlorapatite and merrillite
335 in the GRA 06128/9 achondrites (Shearer et al., 2011), although intergrowth was also

Always consult and cite the final, published document. See http:/www.minsocam.org or GeoscienceWorld

This is the peer-reviewed, final accepted version for American Mineralogist, published by the Mineralogical Society of America.
The published version is subject to change. Cite as Authors (Year) Title. American Mineralogist, in press.
DOI: https://doi.org/10.2138/am-2022-8712. http://www.minsocam.org/

proposed as an alternative (e.g., Day et al., 2012). Hyde et al. (2014) reported that merrillite is present along the edges of some of the chlorapatite grains in the NWA 4872 brachinite. However, they proposed that the merrillite is magmatic in origin and that the chlorapatite formed from a reaction between merrillite and a Cl-rich melt residuum or lower-temperature fluids on the parent body (Hyde et al., 2014).

In NWA 4969 and NWA 11756, merrillite always occurs along the edges of the intergranular apatite grains or penetrates the interior of the apatite grains, similar to the texture of intergranular Ca-phosphate minerals in NWA 4872 (Hyde et al., 2014). Particularly, in NWA 4969, many intergranular apatite grains are partly or completely enclosed by porous merrillite. Although such a texture is consistent with a replacement origin, it is contrary with the interpretation that apatite formed by reaction between merrillite and Cl-rich fluids (Hyde et al., 2014). In typical replacement textures, secondary mineral or mineral assemblage usually encloses the relict primary mineral or penetrates into the fractures in primary mineral (e.g., Putnis, 2002, 2009; Altree-Williams et al., 2015; Harlov, 2015). Therefore, it is more likely that the intergranular apatite grains were partly replaced by merrillite along the interface with the surrounding silicate minerals or fractures in the original apatite grains. In NWA 4969, small pores in merrillite occur only in regions adjacent to the interface with apatite. The apatite grains are themselves free of pores. Such textures also support the idea that apatite was replaced by merrillite, since porous textures always develop in the reaction products that form through coupled dissolution-

Always consult and cite the final, published document. See http:/www.minsocam.org or GeoscienceWorld

This is the peer-reviewed, final accepted version for American Mineralogist, published by the Mineralogical Society of America.
The published version is subject to change. Cite as Authors (Year) Title. American Mineralogist, in press.
DOI: https://doi.org/10.2138/am-2022-8712. http://www.minsocam.org/

356 reprecipitation in natural and experimental replaced samples (e.g., Putnis, 2002, 2009;
357 Altree-Williams et al., 2015; Harlov, 2015). The formation of small pores could be related
358 to volume change and/or mass transfer during replacement (Putnis, 2002; Putnis and John,
359 2010). Since the replacement of chlorapatite by merrillite is a devolatilization reaction, Cl-
360 rich fluids, most likely as vapors, were probably lost along the grain boundaries or via the
361 porosity. In addition, the similar REE patterns between intergranular apatite and associated
362 merrillite and the small difference in their concentration in NWA 4969 also support the idea
363 that the intergranular apatite was replaced by merrillite.

364 To our knowledge, no experiments studying the transformation from chlorapatite to
365 merrillite have been reported yet. However, previous investigations involving synthesis
366 and thermal stability of hydroxyapatite and chlorapatite can provide some insights into the
367 replacement of apatite by merrillite in the present study. For instance, Demnati et al. (2012)
368 found that pure chlorapatite powder has a good thermal stability over a large temperature
369 range (30–1400 ^{o}C). This result is consistent with the experiments by Adolfsson and
370 Hermansson (2000) that no phase changes were detected in the hot isostatically pressed
371 Al_2O_3-apatite composites. However, Adolfssonn and Hermansson (2000) found that
372 chlorapatite may first react with the moisture in the air and partly convert to
373 oxyhydroxyapatite and then react with Al_2O_3 to form $Ca_3(PO_4)_2$ and $CaAl_2O_4$, if the Al_2O_3-
374 apatite composites were crushed and heat-treated in air. Jang et al. (2015) reported that the
375 presence of Mg^{2+} ions in relatively low-pH solutions may facilitate the transformation from

Always consult and cite the final, published document. See http:/www.minsocam.org or GeoscienceWorld

This is the peer-reviewed, final accepted version for American Mineralogist, published by the Mineralogical Society of America.
The published version is subject to change. Cite as Authors (Year) Title. American Mineralogist, in press.
DOI: https://doi.org/10.2138/am-2022-8712. http://www.minsocam.org/

hydroxyapatite to whitlockite, an isomorphous mineral of merrillite, consistent with the observations in Hughes et al. (2008). These experimental results indicate that some minor contaminants in open systems may decrease the thermal stability of chlorapatite and facilitate the formation of whitlockite/merrillite (Hughes et al., 2008). As it will be discussed in the following section, formation of pyroxene-troilite intergrowths in brachinites involves the sulfidization of olivine (Goodrich et al., 2017), which releases minor Mg and Fe. Since the apatite-merrillite assemblage is spatially associated with the pyroxene-troilite intergrowth, therefore, it is likely that the release of Mg and Fe during sulfidization of olivine facilitates the replacement of chlorapatite by merrillite.

We note that Hughes et al. (2008) and Jang et al. (2015) obtained whitlockite in solutions at 240 ºC and 70 ºC, respectively. If the replacement of apatite by merrillite in brachinites also occurred in solutions at similar temperatures, alteration of olivine to serpentine would be expected to be present. However, no serpentine was observed in either the present study or in previous investigations (e.g., Hyde et al., 2014). This implies that the replacement of apatite by merrillite should take place without aqueous solutions, probably at high temperatures, which is consistent with the high temperatures required for the sulfidization of olivine.

Sulfidization of olivine in brachinites

Pyroxene-troilite intergrowths have been observed in many brachinites (e.g., Rumble

Always consult and cite the final, published document. See http:/www.minsocam.org or GeoscienceWorld

This is the peer-reviewed, final accepted version for American Mineralogist, published by the Mineralogical Society of America.
The published version is subject to change. Cite as Authors (Year) Title. American Mineralogist, in press.
DOI: https://doi.org/10.2138/am-2022-8712. http://www.minsocam.org/

et al., 2008; Goodrich et al., 2011, 2017; Singerling et al., 2013; Day et al., 2019). They were interpreted to have resulted from the sulfidization of olivine based on the intergrowth texture (Singerling et al., 2013; Goodrich et al., 2017): $2(Fe,Mg)_2SiO_4 + S_2(g) \leftrightarrow 2MgSiO_3 + 2FeS + O_2(g)$. The same mechanism was also proposed to account for the replacement of olivine by orthopyroxene and troilite in the Apollo lunar samples (Colson, 1992; Norman et al., 1995; Shearer et al., 2012), HED meteorites (Zhang et al., 2018, 2020), and in the ungrouped achondrite Divnoe (Petaev et al., 1994). However, as Goodrich et al. (2017) pointed out, the above reaction equation is too simplistic. If considering the specific compositions of relict olivine and the orthopyroxene in the intergrowths, Si would be somehow gained or Mg and Fe would be released from the system (c.f., Shearer et al., 2012; Zhang et al., 2018). In addition, the presence of troilite in the intergrowths indicates that the S fugacity should be buffered by the reaction $FeS \leftrightarrow Fe + 1/2\ S_2$ (Shearer et al., 2012; Zhang et al., 2018). This reaction can also account for the presence of minor amounts of Fe-metal in the intergrowths (Shearer et al., 2012; Zhang et al., 2018, 2020).

In the present study, the three brachinites contain pyroxene-troilite intergrowths in various abundances along olivine grain boundaries. Their textures resemble those described in other brachinites (Rumble et al., 2008; Goodrich et al., 2011, 2017; Day et al., 2019). In NWA 10637 and NWA 11756, the small orthopyroxene grains in the intergrowths contain Al_2O_3, TiO_2, and Cr_2O_3, which is systematically lower than that in intergranular orthopyroxene (Fig. 7). Although NWA 4969 contains no intergranular orthopyroxene, the

Always consult and cite the final, published document. See http:/www.minsocam.org or GeoscienceWorld

This is the peer-reviewed, final accepted version for American Mineralogist, published by the Mineralogical Society of America.
The published version is subject to change. Cite as Authors (Year) Title. American Mineralogist, in press.
DOI: https://doi.org/10.2138/am-2022-8712. http://www.minsocam.org/

orthopyroxene grains in the intergrowths contain similarly low Al_2O_3, TiO_2, and Cr_2O_3 contents to those in NWA 10637 and NWA 11756 (Fig. 7). This Al-Ti-Cr-poor feature of orthopyroxene has also been reported for orthopyroxene in the intergrowths from Divnoe, Apollo lunar samples, and HED meteorites, as an important indicator for the sulfidization origin of pyroxene-troilite intergrowths (Petaev et al., 1994; Shearer et al., 2012; Zhang et al., 2018, 2020). Therefore, the relatively Al,Ti,Cr-poor feature in the present study supports the idea that the pyroxene-troilite intergrowths in brachinites are sulfidization products of olivine (Goodrich et al., 2017).

One of the important observations in the present study is that the pyroxene-troilite intergrowths in brachinites contain not only orthopyroxene but also high-Ca pyroxene, although high-Ca pyroxene is much less abundant than orthopyroxene. The fine high-Ca pyroxene grains in the pyroxene-troilite intergrowths also have Al_2O_3, Cr_2O_3, and TiO_2 contents systematically lower than the intergranular high-Ca pyroxene (Fig. 6). Al,Ti,Cr-poor high-Ca pyroxene was not observed in the pyroxene-troilite intergrowths described in the Divnoe, Apollo lunar samples, and HED meteorites (e.g., Petaev et al., 1994; Shearer et al., 2012; Zhang et al., 2018, 2020). They were also not reported in previous investigations on brachinites, probably due to their low modal abundance and the difficulty of distinguishing them from the dominant orthopyroxene under BSE imaging. The low contents of Al_2O_3, Cr_2O_3, and TiO_2, compared with intergranular high-Ca pyroxene, imply that the fine-grained high-Ca pyroxene in the intergrowths should be a byproduct during

Always consult and cite the final, published document. See http:/www.minsocam.org or GeoscienceWorld

This is the peer-reviewed, final accepted version for American Mineralogist, published by the Mineralogical Society of America.
The published version is subject to change. Cite as Authors (Year) Title. American Mineralogist, in press.
DOI: https://doi.org/10.2138/am-2022-8712. http://www.minsocam.org/

436 sulfidization of the olivine. Since olivine in brachinites is a Ca-poor phase, the presence of
437 minor high-Ca pyroxene in the intergrowths indicates the addition of external Ca to the
438 system. Because the transformation from apatite (Ca/P~1.67) to merrillite (Ca/P~1.29)
439 releases Ca, this would suggest that the apatite-merrillite transformation supplies the
440 necessary Ca for the formation of Al-Ti-Cr-poor high-Ca pyroxene in the pyroxene-troilite
441 intergrowth. The addition of Ca could also account for the similarity between the Wo
442 components in the intergranular orthopyroxene and the fine-grained orthopyroxene in the
443 intergrowth. For comparison, the fine-grained orthopyroxene in the intergrowth from
444 diogenites and the Apollo lunar samples contains a lower Wo component than those
445 crystallized from mafic to ultramafic magmas (Shearer et al., 2012; Zhang et al., 2018,
446 2020). If this is correct, the apatite-merrillite transformation and the sulfidization of olivine
447 in brachinites could be coupled during a common heating event. The release of Mg and Fe
448 during sulfidization of olivine facilitates the apatite-merrillite transformation; meanwhile,
449 the release of Ca during apatite-merrillite transformation results in the formation of high-
450 Ca pyroxene in the pyroxene-troilite intergrowth. The presence of orthopyroxene + high-
451 Ca pyroxene assemblage instead of pigeonite is probably due to the instability of pigeonite
452 in the presence of a S-rich vapor (Kullerud and Yoder, 1963; Zhang et al., 2013; Wang et
453 al., 2019). Based on temperatures estimated from the paired orthopyroxene and high-Ca
454 pyroxene in the intergrowths, the heating event probably took place at around 930 to
455 1000 °C, which is consistent with the high temperatures required for sulfidization of silicate

Always consult and cite the final, published document. See http:/www.minsocam.org or GeoscienceWorld

This is the peer-reviewed, final accepted version for American Mineralogist, published by the Mineralogical Society of America.
The published version is subject to change. Cite as Authors (Year) Title. American Mineralogist, in press.
DOI: https://doi.org/10.2138/am-2022-8712. http://www.minsocam.org/

456 minerals (Kullerud and Yoder, 1963).

457 In brachinites, the pyroxene-troilite intergrowths are present only along olivine grain
458 boundaries (Rumble et al., 2008; Singerling et al., 2013; Goodrich et al., 2017; this study).
459 This textural feature indicates that the S-rich material reacting with olivine must have been
460 able to permeate the rock along the olivine grain boundaries. The most likely phase that
461 could cause these features is a S-rich vapor. In the previous investigations that studied
462 sulfidization of olivine and pyroxene, two potential mechanisms have been proposed to
463 account for the generation of S-rich vapors: (1) Degassing during magma emplacement
464 may generate S-rich vapors (Shearer et al., 2012); and (2) Impact events may remobilize S
465 in projectile or target materials (Zhang et al., 2013; Goodrich et al., 2017; Wang et al.,
466 2019). Goodrich et al. (2017) argued that generation of S-rich vapors in the parent bodies
467 of brachinites and brachinite-like achondrites cannot be explained by magma degassing
468 during magma emplacement, considering the difficulty of generating multiple melting
469 events on a primitive achondrite parent body. Therefore, they suggested that the S-rich
470 vapors would be generated elsewhere by impact events and migrate into the brachinites
471 and brachinite-like achondrites (Goodrich et al., 2017). In the present study, we concur that
472 impact-induced formation mechanism was the most likely source of S-rich vapors.
473 However, the observations in this study cannot totally exclude the possibility that impact-
474 induced S-rich vapor had a local source since brachinites themselves contain sulfide grains.
475 This takes into account that S is readily remobilized along heated grain boundaries during

Always consult and cite the final, published document. See http:/www.minsocam.org or GeoscienceWorld

This is the peer-reviewed, final accepted version for American Mineralogist, published by the Mineralogical Society of America.
The published version is subject to change. Cite as Authors (Year) Title. American Mineralogist, in press.
DOI: https://doi.org/10.2138/am-2022-8712. http://www.minsocam.org/

476 shock metamorphism (Sharp and DeCarli, 2006).

477

478 **Exsolution of chromite in apatite**

479 The present study shows that almost all the apatite grains in the three brachinites
480 contain oriented tiny or acicular chromite grains. To our knowledge, this is the first
481 description about acicular chromite inclusions within apatite. Harlov (2015) reported
482 monazite and/or xenotime inclusions in reacted apatite grains, with the unreacted apatite
483 grains themselves containing no such inclusions. They proposed that the inclusions formed
484 via coupled dissolution-reprecipitation with fluids (Harlov, 2015). However, this scenario
485 cannot account for the presence of acicular chromite inclusions in both the relict
486 intergranular apatite grains and the apatite inclusions within chromite (Figs. 2 and 3).
487 Instead, the textural correlation between tiny chromite grains and host/surrounding apatite
488 grains resembles the occurrences of subparallel acicular chromite within Fe-rich olivine
489 and of chromite surrounding olivine in weakly metamorphosed ordinary chondrites
490 (L3.1/3.2), which was proposed to be an exsolution product of chromite from olivine
491 (Grossman and Brearley, 2005). Based on the textural similarity, we suggest that the
492 parallel acicular chromite grains could be an exsolution product from originally Cr-bearing
493 chlorapatite. However, no phase diagram exists showing the relationship between chromite
494 and apatite, although Cr^{3+} is expected to be present in the apatite structure (Maunaye et al.,
495 1976; Pan and Fleet, 2002; Hughes and Rakovan, 2015). There is no information on

Always consult and cite the final, published document. See http:/www.minsocam.org or GeoscienceWorld

This is the peer-reviewed, final accepted version for American Mineralogist, published by the Mineralogical Society of America.
The published version is subject to change. Cite as Authors (Year) Title. American Mineralogist, in press.
DOI: https://doi.org/10.2138/am-2022-8712. http://www.minsocam.org/

496 diffusion rates of Cr and Fe in apatite in the literature. Therefore, it is difficult to directly
497 constrain the exsolution temperature and duration of chromite precipitation from the apatite.
498 However, if the heating event lasted for a long time at high temperature, relatively coarse
499 discrete chromite grains due to Ostwald ripening, rather than tiny grains, would be expected
500 to occur, especially along the grain boundaries between apatite and the surrounding silicate
501 phases. Considering that a heating event occurred responsible for the apatite replacement
502 by merrillite and sulfidization of olivine, the exsolution of chromite in apatite could be
503 another product of the transient heating event on the brachinite parent body.
504
505 **Relict origin of apatite inclusions within silicate and chromite**
506 Apatite is observed as inclusions within silicate and chromite from all three
507 brachinites in this study. They either occur as individual grains or are associated with pore-
508 free merrillite grains. Some merrillite grains occur as subhedral-euhedral grains included
509 in the apatite inclusions. The apatite inclusions are distinctly different from those of the
510 intergranular apatite and have two aspects of significance. First, most, if not all, of the
511 apatite inclusions were probably protected by host chromite and silicate minerals and
512 escaped replacement by merrillite. Second, most of the merrillite grains should have
513 formed simultaneously with their host apatite grains, rather than be a replacement product
514 of the latter.
515 Apatite inclusions have been reported in a few brachinites (Brachina, Nehru et al.,

Always consult and cite the final, published document. See http:/www.minsocam.org or GeoscienceWorld

This is the peer-reviewed, final accepted version for American Mineralogist, published by the Mineralogical Society of America.
The published version is subject to change. Cite as Authors (Year) Title. American Mineralogist, in press.
DOI: https://doi.org/10.2138/am-2022-8712. http://www.minsocam.org/

516 1983) and brachinite-like achondrites (MIL 090340, Goodrich et al., 2017). However, the
517 origin of the apatite inclusions was not discussed. Day et al. (2019) argued that formation
518 of phosphate inclusions within olivine in brachinites and brachinite-like achondrites could
519 be related to the refertilization effect of a late-stage melt. However, the refertilization
520 scenario cannot account for the textural and compositional features of the apatite and
521 olivine inclusions within chromite in NWA 4969. First, chromite is a highly refractory
522 mineral during partial melting (Arai, 1994). It is unlikely that a chromite grain of residual
523 origin includes phases that crystallized from late-stage refertilization melts. Second, the
524 apatite inclusions within chromite from NWA 4969 are more F-rich than the intergranular
525 apatite in the same sample. This observation contrasts with the expectation from the
526 refertilization scenario that both the intergranular apatite and apatite inclusions would have
527 similar chemical compositions. Third, if the olivine inclusion within chromite is genetically
528 the same as the apatite inclusion within chromite, its higher Mg# also contrasts with the
529 expected behavior that the equigranular olivine and the olivine inclusion would have
530 similar compositions.

531 The above discussion suggests that apatite inclusions within chromite from
532 brachinites (at least NWA 4969) cannot be a product of late-stage melt refertilization.
533 Instead, the apatite inclusion (and associated merrillite), along with the intergranular apatite,
534 probably formed under different processes and the former should have formed earlier than
535 the latter. One may propose a possibility that apatite and olivine inclusions in brachinites

Always consult and cite the final, published document. See http:/www.minsocam.org or GeoscienceWorld

This is the peer-reviewed, final accepted version for American Mineralogist, published by the Mineralogical Society of America.
The published version is subject to change. Cite as Authors (Year) Title. American Mineralogist, in press.
DOI: https://doi.org/10.2138/am-2022-8712. http://www.minsocam.org/

have a magmatic origin and are the earliest crystallizing phases from a mafic or ultramafic melt, given that some brachinites have been suggested to be cumulates (e.g., Warren and Kallemeyn, 1989; Mittlefehldt et al., 2003). The observation that the olivine inclusions within chromite from NWA 4969 are more magnesian than the intergranular olivine seems to be consistent with this possibility. However, this scenario does not explain the early crystallization of apatite inclusions within chromite and their associated merrillite, because Ca-phosphate minerals are typically late-stage crystallization phases in basaltic melts (Watson, 1980). Therefore, the phosphate inclusions within chromite from the brachinites are not magmatic in origin although we cannot exclude the possibility that the host brachinites might be cumulate.

We propose that the apatite inclusions in brachinites could be relicts from the precursor materials of brachinites, while the intergranular apatite grains could be attributed to late-stage melt refertilization, following the idea that most brachinites are partial melt residues (e.g., Day et al., 2019; references therein). A relict origin for the apatite inclusion can readily account for the presence of rare fluorapatite in NWA 4969, given that most intergranular apatite grains in brachinites are chlorapatite. If apatite crystallizes from a common Cl-rich, F-bearing melt, no fluorapatite grains would be expected to occur, given that the other minerals are chemically homogeneous. This is contrary with observation. Similarly, such a scenario can also explain why intergranular apatite grains are not present in NWA 10637, but apatite inclusions are relatively common. We suspect that the apatite

Always consult and cite the final, published document. See http:/www.minsocam.org or GeoscienceWorld

This is the peer-reviewed, final accepted version for American Mineralogist, published by the Mineralogical Society of America.
The published version is subject to change. Cite as Authors (Year) Title. American Mineralogist, in press.
DOI: https://doi.org/10.2138/am-2022-8712. http://www.minsocam.org/

556 inclusions and associated phases within the chromite and olivine may have been prevented
557 from partial melting or isolated from melts due to the protection of refractory chromite or
558 silicate minerals, although Ca-phosphate minerals are less refractory than chromite and
559 olivine (Watson, 1980). However, based on the current observations, it is difficult to
560 constrain the properties of potential precursor(s).
561

562 **Comparison of apatite between brachinites and other meteorites**

563 McCubbin and Jones (2015) and Ward et al. (2017) have compared the halogen
564 compositions of apatite in different extraterrestrial materials. Apatite halogen compositions
565 can be divided into three broad groups. (1) Apatite from ordinary chondrites, carbonaceous
566 chondrites, and the achondrites GRA 06128/9 is mainly chlorapatite, although some apatite
567 grains in carbonaceous chondrites are halogen-poor hydroxyapatite (Piralla et al., 2021 and
568 references therein). (2) Apatite in Martian meteorites has a large variation in composition,
569 almost covering the whole space in the Cl-F-OH ternary (McCubbin and Jones, 2015;
570 McCubbin et al., 2016). (3) Apatite from other achondrites (eucrites, winonaites, and
571 acapulcoites) and lunar samples (Apollo samples and lunar meteorites) is mainly
572 fluorapatite. Lastly, some apatite grains from ureilitic trachyandesite ALM-A contain equal
573 amounts of chlorapatite and fluorapatite components (Ward et al., 2017). Ward et al. (2017)
574 also studied the trace element compositions of Ca-phosphate minerals in different
575 meteorites and found a large variation in the REE, U, and Th compositions among different

Always consult and cite the final, published document. See http:/www.minsocam.org or GeoscienceWorld

This is the peer-reviewed, final accepted version for American Mineralogist, published by the Mineralogical Society of America.
The published version is subject to change. Cite as Authors (Year) Title. American Mineralogist, in press.
DOI: https://doi.org/10.2138/am-2022-8712. http://www.minsocam.org/

576 groups of meteorites.

577 GRA 06128/9 are a pair of plagioclase-dominant achondrites that were suggested to
578 be genetically associated with brachinites (Shearer et al., 2008, 2010; Day et al., 2009,
579 2012). Apatite is also an important accessory mineral in these meteorites (Day et al., 2009,
580 2012; Shearer et al., 2010, 2011; McCubbin and Jones, 2015; Zhou et al., 2018). Apatite
581 from GRA 06128/9 and brachinites are similar in two ways. First, both the apatite in GRA
582 06128/9 and the intergranular apatite in brachinites are chlorapatite, although the
583 intergranular apatite in brachinites displays a much larger variation in the halogen
584 composition and a higher OH/Other anion components than those in GRA 06128/9 (Fig.
585 8a). Second, apatite from GRA 06128/9 has REE patterns and concentrations comparable
586 to those of intergranular apatite in brachinites, although LREE in GRA 06128/9 apatite are
587 relatively enriched compared to HREE (Fig. 9). However, there are two major differences
588 for apatite and associated merrillite between GRA 06128/9 and brachinites. First, the
589 apatite-merrillite texture in GRA 06128/9 distinctly differs from that of the intergranular
590 apatite and merrillite in the brachinites. In GRA 06128/9, chlorapatite replaced or intergrew
591 with merrillite (Shearer et al., 2011; Day et al., 2012; Zhou et al., 2018). In contrast, in the
592 brachinites, intergranular chlorapatite was replaced by merrillite (this study). This
593 distinction indicates different or even opposite halogen behaviors between GRA 06128/9
594 and the brachinites. Second, merrillite and apatite in GRA 06128/9 have different REE
595 patterns (including different Eu anomalies). The REE concentrations in merrillite are

Always consult and cite the final, published document. See http:/www.minsocam.org or GeoscienceWorld

This is the peer-reviewed, final accepted version for American Mineralogist, published by the Mineralogical Society of America.
The published version is subject to change. Cite as Authors (Year) Title. American Mineralogist, in press.
DOI: https://doi.org/10.2138/am-2022-8712. http://www.minsocam.org/

596 higher by one order of magnitude than those in apatite (Shearer et al., 2010; Fig. 9).
597 However, intergranular merrillite in brachinites has a REE pattern similar to that of the
598 intergranular apatite (Fig. 9).

599 Based on the studies of McCubbin and Jones (2015) and Ward et al. (2017), apatite in
600 chondrites has halogen compositions that are different from those in most achondrites
601 (winonaites, acapulcoites, eucrites) and lunar samples. Interestingly, the Cl-rich feature of
602 apatite in brachinites and GRA 06128/9 is similar to that in chondrites (Cl-rich) rather than
603 other achondrites (F-rich), even primitive achondrites (winonaites and acapulcoites).
604 Furthermore, the low concentrations of U and Th and the small positive Eu anomaly also
605 resemble that found in apatite from chondrites (especially less metamorphosed chondrites)
606 rather than achondrites (Figs. 9 and 10; Zhang et al., 2016; Ward et al., 2017; Zhou et al.,
607 2018). If all achondrites have a chondritic parent body, these similarities for apatite imply
608 that brachinites probably retained the chemical features of their chondritic precursors more
609 completely than other achondrites (e.g., eucrites, winonaites, and acapulcoites) and lunar
610 samples. From this point of view, brachinites are a unique material that probably witnessed
611 the earliest stage evolution of the achondrite parent body.

612

613 ## IMPLICATIONS

614 In the present study, two types of apatite in brachinites were observed: intergranular
615 apatite and apatite inclusion within other minerals. Here intergranular chlorapatite in

Always consult and cite the final, published document. See http:/www.minsocam.org or GeoscienceWorld

This is the peer-reviewed, final accepted version for American Mineralogist, published by the Mineralogical Society of America.
The published version is subject to change. Cite as Authors (Year) Title. American Mineralogist, in press.
DOI: https://doi.org/10.2138/am-2022-8712. http://www.minsocam.org/

616 brachinites was replaced by merrillite, indicating halogen devolatilization on the brachinite
617 parent body. This type of halogen devolatilization behavior has not been reported in the
618 literature yet and differs from many previous investigations that proposed replacement of
619 merrillite by Cl-rich fluids on the asteroids and Mars. If an impact event was responsible
620 for the devolatilization of halogen in brachinites, similar behavior probably takes place on
621 other asteroids, the Moon, and even terrestrial planets, since impact is one of the
622 fundamental processes during planetary evolution.

623 Mn-Cr isotope systematics are very useful for the geochronology of the early solar
624 system (Birck and Allègre, 1988; Krot et al., 2006). However, one of the prerequisites of
625 applying this chronological method is that the Mn-Cr system should be closed. Otherwise,
626 the Mn-Cr age may be related to post-formation heating events or else be meaningless.
627 Here fine chromite grains exsolved from apatite, indicating that Cr was probably locally or
628 totally re-equilibrated among the different minerals during the heating event. If this is the
629 case, the Cr isotopic compositions of different minerals in the brachinites are expected to
630 have been disturbed or reset. For example, Dunlap et al. (2016a) obtained a young Mn-Cr
631 age (4550.2 ± 0.8 Ma) for NWA 4882, which suggested a protracted thermal history (most
632 likely from impact heating) on the brachinite parent body.

633 The large variation in halogen composition in an apatite aggregate (~40 μm) included
634 in chromite from NWA 4969 (including the presence of fluorapatite) is a striking feature in
635 this study. Such a large compositional variation has not been reported in metamorphic and

Always consult and cite the final, published document. See http:/www.minsocam.org or GeoscienceWorld

This is the peer-reviewed, final accepted version for American Mineralogist, published by the Mineralogical Society of America.
The published version is subject to change. Cite as Authors (Year) Title. American Mineralogist, in press.
DOI: https://doi.org/10.2138/am-2022-8712. http://www.minsocam.org/

igneous apatite from chondrites, eucrites, and primitive achondrites, although some apatite grains in ordinary chondrites, affected by impact-induced melting, exhibit a large variation in F and Cl abundances (Jones et al., 2016; Li and Hsu, 2018; Wu and Hsu, 2019). This implies that the halogen evolution of the brachinite parent body should be very complex and largely different from other primitive achondrites.

ACKNOWLEDGEMENTS

We thank Prof. Rhian H. Jones and an anonymous reviewer for their constructive and helpful comments and Dr. Daniel Harlov for his editorial effort. This study was financially supported by National Natural Science Foundation of China (42025302, 41973061), the B-type Strategic Priority Program of the Chinese Academy of Sciences (XDB41000000), and the pre-research Project on Civil Aerospace Technologies funded by CNSA (D020204).

Always consult and cite the final, published document. See http:/www.minsocam.org or GeoscienceWorld

This is the peer-reviewed, final accepted version for American Mineralogist, published by the Mineralogical Society of America.
The published version is subject to change. Cite as Authors (Year) Title. American Mineralogist, in press.
DOI: https://doi.org/10.2138/am-2022-8712. http://www.minsocam.org/

REFERENCES CITED

Adolfsson, E., and Hermansson, L. (2000) Phase stability aspects of various apatite-aluminum oxide composites. Journal of Materials Science, 35, 5719–5723.

Altree-Williams, A., Pring, A., Ngothai, Y., and Brügger, J. (2015) Textural and compositional complexities resulting from coupled dissolution–reprecipitation reactions in geomaterials. Earth-Science Reviews, 150, 628–651.

Arai, S. (1994) Characterization of spinel peridotites by olivine-spinel compositional relationships: review and interpretation. Chemical Geology, 113, 191–204.

Barrat, J. A., Zanda, B., Moynier, F., Bollinger, C., Liorzou, C., and Bayon, G. (2012) Geochemistry of CI chondrites: Major and trace elements, and Cu and Zn isotopes. Geochimica et Cosmochimica Acta, 83, 79–92.

Beard, S. P., Swindle, T. D., and Isachsen, C. (2016) Ar-Ar ages of brachinite and brachinite-like achondrites. 79th Annual Meeting of the Meteoritical Society. Abstract #6411.

Birck, J.-L., and Allègre, C. J. (1988) Manganese-chromium isotope systematics and the development of the early solar system. Nature, 331, 579–584.

Bouvier, A., Gattacceca, J., Grossman, J., and Metzler, K. (2017) The Meteoritical Bulletin, No. 105. Meteoritics & Planetary Science, 52. doi.org/10.1111/maps.12944.

Always consult and cite the final, published document. See http:/www.minsocam.org or GeoscienceWorld

This is the peer-reviewed, final accepted version for American Mineralogist, published by the Mineralogical Society of America.
The published version is subject to change. Cite as Authors (Year) Title. American Mineralogist, in press.
DOI: https://doi.org/10.2138/am-2022-8712. http://www.minsocam.org/

667 Brearley, A. J., and Jones, R. H. (2018) Halogens in chondritic meteorites. In The Role of
668 halogens in terrestrial and extraterrestrial geochemical processes (edited by Harlov,
669 D. E., and Aranovich, L.) Springer Geochemistry. 871–958.
670 Brey, G. P., and Kohler, T. (1990) Geothermobarometry in four-phase lherzolites II: new
671 thermobarometers, and practical assessment of existing thermobarometers. Journal of
672 Petrology, 31, 1353–1378.
673 Collinet, M., and Grove, T. L. (2020) Widespread production of silica- and alkali-rich melts
674 at the onset of planetesimal melting. Geochimica et Cosmochimica Acta, 277, 334–
675 357.
676 Colson, R. O. (1992) Mineralization on the Moon? Theoretical considerations of Apollo
677 16 “rusty rocks”, replacement in 67016, and surface-correlated volatiles on lunar
678 volcanic glass. Proceedings 22nd Lunar and Planetary Science Conference. 427–436.
679 Crossley, S. D., Ash, R. D., Sunshine, J. M., Corrigan, C. M., McCoy, T. J., Mittlefehldt,
680 D. W., and Puchtel, I. S. (2020) Sulfide-dominated partial melting pathways in
681 brachinites. Meteoritics & Planetary Science, 55, 2021–2043.
682 Connolly, H. C., Smith, C., Benedix, G., Folco, L., Righter, K., Zipfel, J., Yamaguchi, A.,
683 and Chennaoui Aoudjehane, H. (2008) The Meteoritical Bulletin, No. 93, 2008 March.
684 Meteoritics & Planetary Science, 43, 571–632.

Always consult and cite the final, published document. See http:/www.minsocam.org or GeoscienceWorld

This is the peer-reviewed, final accepted version for American Mineralogist, published by the Mineralogical Society of America.
The published version is subject to change. Cite as Authors (Year) Title. American Mineralogist, in press.
DOI: https://doi.org/10.2138/am-2022-8712. http://www.minsocam.org/

685 Day, J. M. D., Ash, R. D., Liu, Y., Bellucci, J. J., Rumble, D., McDonough, W. F., Walker,
686 R. J., and Taylor, L. A. (2009) Early formation of evolved asteroidal crust. Nature,
687 457, 179–182.
688 Day, J. M. D., Walker, R. J., Ash, R. D., Liu, Y., Rumble, D., Irving, A. J., Goodrich, C.
689 A., Tait, K., McDonough, W. F., and Taylor, L. A. (2012) Origin of felsic achondrites
690 Graves Nunataks 06128 and 06129, and ultramafic brachinites and brachinite-like
691 achondrites by partial melting of volatile-rich primitive parent bodies. Geochimica et
692 Cosmochimica Acta, 81, 94–128.
693 Day, J. M. D., Corder, C. A., Rumble, D., Assayag, N., Cartigny, P., and Taylor, L. A.
694 (2015) Differentiation processes in FeO-rich asteroids revealed by the achondrite
695 Lewis Cliff 88763. Meteoritics & Planetary Science, 50, 1750–1766
696 Day, J. M. D., Corder, C. A., Assayag, N., and Cartigny, P. (2019) Ferrous oxide-rich
697 asteroid achondrites. Geochimica et Cosmochimica Acta, 266, 544–567.
698 Demnati, I., Grossin, D., Combes, C., Parco, M., Braceras, I., and Rey, C. (2012) A
699 comparative physico-chemical study of chlorapatite and hydroxyapatite: from
700 powders to plasma sprayed thin coatings. Biomedical Materials, 7, 054101.
701 Dunlap, D. R., Romaniello, S. J., and Wadhwa, M. (2016a) ^{53}Mn-^{53}Cr systematics of the
702 brachinite NWA 4882. 79th Annual Meeting of the Meteoritical Society. Abstract
703 #6217.

Always consult and cite the final, published document. See http:/www.minsocam.org or GeoscienceWorld

This is the peer-reviewed, final accepted version for American Mineralogist, published by the Mineralogical Society of America.
The published version is subject to change. Cite as Authors (Year) Title. American Mineralogist, in press.
DOI: https://doi.org/10.2138/am-2022-8712. http://www.minsocam.org/

Dunlap, D. R., Wadhwa, M., and Romaniello, S. J. (2016b) ^{53}Mn-^{53}Cr systematics of brachina revised in high precision. 47th Lunar and Planetary Science Conference. Abstract#3055.

Gardner-Vandy, K. G., Lauretta, D. S., and McCoy, T. J. (2013) A petrologic, thermodynamic and experimental study of brachinites: Partial melt residues of an R chondrite-like precursor. Geochimica et Cosmochimica Acta, 122, 36–57.

Gattacceca, J., McCubbin, F. M., Bouvier, A., and Grossman, J. (2020) Meteoritical Bulletin, No. 107. Meteoritics & Planetary Science, 55, 460–462.

Goodrich, C. A., Wlotzka, F., Ross, D. K., and Bartoschewitz, R. (2006) Northwest Africa 1500: Plagioclase-bearing monomict ureilite or ungrouped achondrite? Meteoritics & Planetary Science, 41, 925–952.

Goodrich, C. A., Kita, N. T., Spicuzza, M. J., Valley, J. W., Zipfel, J., Mikouchi, T., and Miyamoto, M. (2011) The Northwest Africa 1500 meteorite: Not a ureilite, maybe a brachinite. Meteoritics & Planetary Science, 45, 1906–1928.

Goodrich, C. A., Kita, N. T., Sutton, S. R., Wirick, S., and Gross, J. (2017) The Miller Range 090340 and 090206 meteorites: Identification of new brachinite-like achondrites with implications for the diversity and petrogenesis of the brachinite clan. Meteoritics & Planetary Science, 52, 949–978.

Grossman, J. N., and Brearley, A. J. (2005) The onset of metamorphism in ordinary and carbonaceous chondrites. Meteoritics & Planetary Science, 40, 87–122.

Always consult and cite the final, published document. See http:/www.minsocam.org or GeoscienceWorld

This is the peer-reviewed, final accepted version for American Mineralogist, published by the Mineralogical Society of America.
The published version is subject to change. Cite as Authors (Year) Title. American Mineralogist, in press.
DOI: https://doi.org/10.2138/am-2022-8712. http://www.minsocam.org/

724 Harlov, D. E. (2015) Apatite: A fingerprint for metasomatic processes. Elements, 11, 171–
725 176.
726 Henderson, C. E. (2011) Beam sensitive in EPMA: The analysis of apatite,
727 $Ca_5(PO_4)_3(F,Cl,OH)$. Microsc. Microanal. 17 (suppl 2), 588–589. Doi:
728 10.1017/S1431927611003813.
729 Howarth, G. H., Pernet-Fisher, J. F., Bodnar, R. J., and Taylor, L. A. (2015) Evidence for
730 the exsolution of Cl-rich fluids in Martian magmas: Apatite petrogenesis in the
731 enriched lherzolitic shergottite Northwest Africa 7755. Geochimica et Cosmochimica
732 Acta, 166, 234–248.
733 Hu, S., Lin, Y., Zhang, J., Hao, J., Xing, W., Zhang, T., Yang, W., and Changela H. (2019)
734 Ancient geologic events on Mars revealed by zircons and apatites from the Martian
735 regolith breccia NWA 7034. Meteoritics & Planetary Science, 54, 850–879.
736 Hughes, J. M., and Rakovan, J. F. (2015) Structurally robust, chemically diverse: apatite
737 and apatite supergroup minerals. Elements, 11, 165–170.
738 Hughes, J. M., Jolliff, B. L., and Rakovan, J. F. (2008) The crystal chemistry of whitlockite
739 and merrillite and the dehydrogenation of whitlockite to merrillite. American
740 Mineralogist, 93, 1300–1305.
741 Hyde, B. C., Day, J. M. D., Tait, K. T., Ash, R. D., Holdsworth, D. W., and Moser, D. E.
742 (2014) Characterization of weathering and heterogeneous mineral phase distribution
743 in brachinite Northwest Africa 4872. Meteoritics & Planetary Science, 49, 1141–1156.

Always consult and cite the final, published document. See http:/www.minsocam.org or GeoscienceWorld

This is the peer-reviewed, final accepted version for American Mineralogist, published by the Mineralogical Society of America.
The published version is subject to change. Cite as Authors (Year) Title. American Mineralogist, in press.
DOI: https://doi.org/10.2138/am-2022-8712. http://www.minsocam.org/

744 Ito, K., Niki, S., Hirata, T., Iizuka, T., and Mikouchi, T. (2022) U-Pb dating of phosphates
745 in the brachinite meteorite Northwest Africa 10932. 53rd Lunar and Planetary Science
746 Conference. Abstract #1744.
747 Jang, H. L., Lee, H. K., Jin, K., Ahn, H. Y., Lee, H. E., and Nam, K. T. (2015) Phase
748 transformation from hydroxyapatite to the secondary bone mineral, whitlockite.
749 Journal of Materials Chemistry B, 3, 1342–1349.
750 Jones, R. H., McCubbin, F. M., Dreeland, L., Guan, Y., Burger, P. V., and Shearer, C. K.
751 (2014) Phosphate minerals in LL chondrites: A record of the action of fluids during
752 metamorphism on ordinary chondrite parent bodies. Geochimica et Cosmochimica
753 Acta, 132, 120–140.
754 Jones, R. H., McCubbin, F. M., and Guan, Y. B. (2016) Phosphate minerals in the H group
755 of ordinary chondrites, and fluid activity recorded by apatite heterogeneity in the Zag
756 H3-6 regolith breccia. American Mineralogist, 101, 2452–2467.
757 Keil, K. (2014) Brachinite meteorites: Partial melt residues from an FeO-rich asteroid.
758 Geochemistry, 74, 311–329.
759 Krot, A. N., Keil, K., Scott, E. R. D., Goodrich, C. A., and Weisberg, M. K. (2014)
760 Classification of meteorites and their genetic relationships. In Meteorites and
761 Cosmochemical processes (Ed. A. M. Davis), Vol. 2 Treatise on Geochemistry, 2nd
762 Ed. (Exec. Eds. H. D. Holland and K. K. Turekian), Elsevier, Oxford, 1–63.

Always consult and cite the final, published document. See http:/www.minsocam.org or GeoscienceWorld

This is the peer-reviewed, final accepted version for American Mineralogist, published by the Mineralogical Society of America.
The published version is subject to change. Cite as Authors (Year) Title. American Mineralogist, in press.
DOI: https://doi.org/10.2138/am-2022-8712. http://www.minsocam.org/

763 Kullerud, G., and Yoder, Jr., H. S. (1963) Sulfide-silicate reactions. Carnegie Institute of
764 Washington Yearbook. Pp. 215–218.
765 Li, S., Hsu, W., Nemchin, A., Che, X., Liu, D., Long, T., Luo, Y., Beard, S., and Tang, C.
766 (2021) Multiple thermal events recorded in IIE silicate inclusions: Evidence from in
767 situ U-Pb dating of phosphates in Weekeroo Station. Geochimica et Cosmochimica
768 Acta, 309, 79–95.
769 Li, Y., and Hsu, W. (2018) Multiple impact events on the L-chondritic parent body:
770 Insights from SIMS U-Pb dating of Ca-phosphates in the NWA 7251 L-melt breccia.
771 Meteoritics & Planetary Science, 53, 1081–1095.
772 Liu, Y. S., Hu, Z. C., Gao, S., Günther, D., Xu, J., Gao, C. G., and Chen, H. H. (2008) In
773 situ analysis of major and trace elements of anhydrous minerals by LA-ICP-MS
774 without applying an internal standard. Chemical Geology, 257, 34–43.
775 Maunaye, M., Hamon, C., L'Haridon, P., and Laurent, Y. (1976) Composés á structure
776 apatite. IV. Étude structural de l'oxynitrure $Sm_8Cr_2Si_6N_2O_{24}$. Bulletin de la Société
777 française de Minéralogie et de Cristallographie, 99, 203–205.
778 McCubbin, F. M., and Jones, R. H. (2015) Extraterrestrial Apatite: Planetary Geochemistry
779 to Astrobiology. Elements, 11, 183–188.
780 McCubbin, F. M., Vander Kaaden, K. E., Tartèse, R., Klim,a R. L., Liu, Y., Mortimer, J.,
781 Barnes, J. J., Shearer, C. K., Treiman, A. H., Lawrence, D. J., Elardo, S. M., Hurley,
782 D. M., Boyce, J. W., and Anand, M. (2015). Magmatic volatiles (H, C, N, F, S, Cl) in

Always consult and cite the final, published document. See http:/www.minsocam.org or GeoscienceWorld

This is the peer-reviewed, final accepted version for American Mineralogist, published by the Mineralogical Society of America.
The published version is subject to change. Cite as Authors (Year) Title. American Mineralogist, in press.
DOI: https://doi.org/10.2138/am-2022-8712. http://www.minsocam.org/

783 the lunar mantle, crust, and regolith: Abundances, distributions, processes, and
784 reservoirs. American Mineralogist, 100, 1668–1707.
785 McCubbin, F. M., Boyce, J. W., Srinivasan, P., Santos, A. R., Elardo, S. M., Filiberto, J.,
786 Steele, A., and Shearer, C. K. (2016) Heterogeneous distribution of H_2O in the
787 Martian interior: Implications for the abundance of H_2O in depleted and enriched
788 mantle sources. Meteoritics & Planetary Science, 51, 2036–2060.
789 McCubbin, F. M., Lewis, J. A., Barnes, J. J., Elardo, S. M., and Boyce, J. W. (2021) The
790 abundance of F, Cl, and H_2O in eucrites: Implications for the origin of volatile
791 depletion in the asteroid 4 Vesta. Geochimica et Cosmochimica Acta, 314, 270–293.
792 Mittlefehldt, D. W., Bogard, D. D., Berkley, J. L., and Garrison, D. H. (2003) Brachinites:
793 Igneous rocks from differentiated asteroid. Meteoritics & Planetary Science, 38,
794 1601–1625.
795 Mittlefehldt, D. W. (2014) Achondrites. In Meteorites and Cosmochemical processes (Ed.
796 A. M. Davis), Vol. 2 Treatise on Geochemistry, 2nd Ed. (Exec. Eds. H. D. Holland
797 and K. K. Turekian), Elsevier, Oxford, 235–266.
798 Nehru, C. E., Prinz, M., Delaney, J. S., Dreibus, G., Palme, H., Spettel, B., and Wänke, H.
799 (1983) Brachina: A new type of meteorite, not a chassignite. Journal of Geophysical
800 Research, 88, B237–B244.

Always consult and cite the final, published document. See http:/www.minsocam.org or GeoscienceWorld

This is the peer-reviewed, final accepted version for American Mineralogist, published by the Mineralogical Society of America.
The published version is subject to change. Cite as Authors (Year) Title. American Mineralogist, in press.
DOI: https://doi.org/10.2138/am-2022-8712. http://www.minsocam.org/

Norman, M. D., and Nemchin, A. A. (2014) A 4.2 billion year old impact basin on the Moon: U-Pb dating of zirconolite and apatite in lunar melt rock 67955. Earth and Planetary Science Letters, 388, 387–398.

Norman, M. D., Keil, K., Griffin, W. L., and Ryan, C. G. (1995) Fragments of ancient lunar crust: petrology and geochemistry of ferroan noritic anorthosites from the Descartes region of the Moon. Geochimica et Cosmochimica Acta, 59, 831–847.

Pan, Y. M., and Fleet, M. E. (2002) Compositions of the apatite-group minerals: substitution mechanisms and controlling factors. Reviews in Mineralogy and Geochemistry, 48, 13–49.

Petaev, M. I., Barsukova, L. D., Lipschutz, M. E., Wang, M. S., Ariskin, A. A., Clayton, R. N., and Mayeda, T. K. (1994) The Divnoe meteorite: petrology, chemistry, oxygen isotopes and origin. Meteoritics, 29, 182–199.

Piralla, M., Tartèse, R., Marrocchi, Y., and Joy, K. H. (2021) Apatite halogen and hydrogen isotope constraints on the conditions of hydrothermal alteration in carbonaceous chondrites. Meteoritics & Planetary Science, 56, 809–828.

Putnis, A. (2002) Mineral replacement reactions: from macroscopic observations to microscopic mechanisms. Mineralogical Magazine, 66, 689–708.

Putnis, A. (2009) Mineral replacement reactions. Reviews in Mineralogy and Geochemistry, 70, 87–124.

Always consult and cite the final, published document. See http:/www.minsocam.org or GeoscienceWorld

This is the peer-reviewed, final accepted version for American Mineralogist, published by the Mineralogical Society of America.
The published version is subject to change. Cite as Authors (Year) Title. American Mineralogist, in press.
DOI: https://doi.org/10.2138/am-2022-8712. http://www.minsocam.org/

Putnis, A., and John, T. (2010) Replacement processes in the Earth's crust. Elements, 6, 159–164.

Rumble, D., Irving, A. J., Bunch, T. E., Wittke, J. H., and Kuehner, S. M. (2008) Oxygen isotopic and petrological diversity among brachinites NWA 4872, NWA 4874, NWA 4882 and NWA 4969: How many ancient parent bodies? Lunar and Planetary Science XXXIX. Abstract #1974.

Sarafian, A. R., Roden, M. F., and Patiño-Douce, A. E. (2013) The volatile content of Vesta: Clues from apatite in eucrites. Meteoritics & Planetary Science, 48, 2135–2154.

Sharp, T. G., and DeCarli, P. S. (2016) Shock effects in meteorites. In Meteorites and the early Solar System II (edited by Lauretta D. S. and McSween Jr. H. Y.). The University of Arizona Press, Tucson. Pp. 653–677.

Shearer, C. K., Burger, P. V., Neal, C. R., Sharp, Z. D., Borg, L. E., Spivak-Birndorf, L., Wadhwa, M., Papike, J. J., Karner, J. M., Gaffney, A. M., Shafer, J., Weiss, B. P., and Geissman, J. (2008) A unique glimpse into asteroidal melting processes in the early solar system from the Graves Nunatak 06128/06129 achondrites. American Mineralogist, 93, 1937–1940.

Shearer, C. K., Burger, P. V., Neal, C. R., Sharp, Z. D., Borg, L. E., Spivak-Birndorf, L., Wadhwa, M., Papike, J. J., Karner, J. M., Gaffney, A. M., Shafer, J., Weiss, B. P., and Geissman, J. (2010) Non-basaltic asteroidal melting during the earliest stages of solar

Always consult and cite the final, published document. See http:/www.minsocam.org or GeoscienceWorld

This is the peer-reviewed, final accepted version for American Mineralogist, published by the Mineralogical Society of America.
The published version is subject to change. Cite as Authors (Year) Title. American Mineralogist, in press.
DOI: https://doi.org/10.2138/am-2022-8712. http://www.minsocam.org/

system evolution. A view from Antarctic achondrites Graves Nunatak 06128 and 06129. Geochimica et Cosmochimica Acta, 74, 1172–1199.

Shearer, C. K., Burger, P. V., Guan, Y., Papike, J. J., Sutton, S. R., and Atudorei, N. V. (2012) Origin of sulfide replacement textures in lunar breccias. Implications for vapor element transport in the lunar crust. Geochimica et Cosmochimica Acta, 83, 138–158.

Shearer, C. K., Burger, P. V., Papike, J. J., Sharp, Z. D., and McKeegan, K. D. (2011) Fluids on differentiated asteroids: Evidence from phosphates in differentiated meteorites GRA 06128 and GRA 06129. Meteoritics & Planetary Science, 46, 1345–1362.

Shearer, C. K., Burger, P. V., Papike, J. J., McCubbin, F. M., and Bell, A. S. (2015) Crystal chemistry of merrillite from Martian meteorites: Mineralogical recorders of magmatic processes and planetary differentiation. Meteoritics & Planetary Science, 50(4), 649–673.

Singerling, S. A., McCoy, T. J., and Gardner-Vandy, K. G. (2013) Possible evidence for sulfidization reactions in the Miller Range brachinites(?). 44th Lunar and Planetary Science Conference. Abstract #1669.

Swindle, T. D., Kring, D. A., Burkland, M. K., Hill, D. H., and Boynton, W. V. (1998) Noble gases, bulk chemistry, and petrography of olivine-rich achondrites Eagles Nest and Lewis Cliff 88763: comparison to brachinites. Meteoritics & Planetary Science, 33, 31–48.

Always consult and cite the final, published document. See http:/www.minsocam.org or GeoscienceWorld

This is the peer-reviewed, final accepted version for American Mineralogist, published by the Mineralogical Society of America.
The published version is subject to change. Cite as Authors (Year) Title. American Mineralogist, in press.
DOI: https://doi.org/10.2138/am-2022-8712. http://www.minsocam.org/

Wadhwa, M., Shukolyukov, A., and Lugmair, W. (1998) ^{53}Mn-^{53}Cr systematics in Brachina: a record of one of the earliest phases of igneous activity on an asteroid. Lunar and Planetary Science XXIX. Abstract #1480.

Wang, S. Z., Zhang, A. C., Pang, R. L., Li, Y., and Chen, J. N. (2019) Possible records of space weathering on Vesta: Case study in a brecciated eucrite Northwest Africa 1109. Meteoritics & Planetary Science, 54, 836–849.

Ward, D., Bischoff, A., Roszjar, J., Berndt, J., and Whitehouse, M. J. (2017) Trace element inventory of meteoritic Ca-phosphates. American Mineralogist, 102, 1856–1880.

Warren, P. H., and Kallemeyn, G. W. (1989) Allan Hills 84025: The second brachinite, far more differentiated than Brachina, and an ultramafic achondritic clast from L chondrite Yamato 75097. Proceedings of 19th Lunar and Planetary Science Conference. Pp. 475–486.

Watson, E. B. (1980) Apatite and phosphorus in mantle source regions: An experimental study of apatite/melt equilibria at pressures at 25 kbar. Earth and Planetary Science Letters, 51, 322–335.

Wu, Y., and Hsu, W. (2019) Petrogenesis and In Situ U-Pb Geochronology of a strongly shocked L-melt rock Northwest Africa 11042. Journal of Geophysical Research: Planets, 124, 893–909.

Yin, Q. Z., Zhou, Q., Li, Q. L., Li, X. H., Liu, Y., Tang, G. Q., Krot, A. N., and Jenniskens, P. (2014) Records of the Moon-forming impact and the 470 Ma disruption of the L

Always consult and cite the final, published document. See http:/www.minsocam.org or GeoscienceWorld

This is the peer-reviewed, final accepted version for American Mineralogist, published by the Mineralogical Society of America.
The published version is subject to change. Cite as Authors (Year) Title. American Mineralogist, in press.
DOI: https://doi.org/10.2138/am-2022-8712. http://www.minsocam.org/

879 chondrite parent body in the asteroid belt from U-Pb apatite ages of Novato.
880 Meteoritics & Planetary Science, 49, 1426–1439.
881 Zhang, A. C., Hsu, W. B., Floss, C., Li, X. H., Li, Q. L., Liu, Y., and Taylor, L. A. (2010)
882 Petrogenesis of lunar meteorite Northwest Africa 2977: Constraints from in situ
883 microprobe results. Meteoritics & Planetary Science, 45, 1929–1947.
884 Zhang, A. C., Wang, R. C., Hsu, W. B., and Bartoschewitz, R. (2013) Record of S-rich
885 vapors on asteroid 4 Vesta: Sulfurization in the Northwest Africa 2339 eucrite.
886 Geochimica et Cosmochimica Acta, 109, 1–13.
887 Zhang, A. C., Li, Q. L., Yurimoto, H., Sakamoto, N., Li, X. H., Hu, S., Lin, Y. T., and
888 Wang, R. C. (2016) Young asteroidal fluid activity revealed by absolute age from
889 apatite in carbonaceous chondrite. Nature Communications, 7, 12844. Doi:
890 10.1038/ncomms12844.
891 Zhang, A. C., Bu, Y. F., Pang, R. L., Sakamoto, N., Yurimoto, H., Chen, L. H., Gao, J. F.,
892 Du, D. H., Wang, X. L., and Wang, R. C. (2018) Origin and implications of troilite-
893 orthopyroxene intergrowths in the brecciated diogenite Northwest Africa 7183.
894 Geochimica et Cosmochimica Acta, 220, 125–145.
895 Zhang, A. C., Kawasaki, N., Bao, H., Liu, J., Qin, L., Kuroda, M., Gao, J. F., Chen, L. H.,
896 He, Y., Sakamoto, N., and Yurimoto, H. (2020) Evidence of metasomatism in the
897 interior of Vesta. Nature Communications, 11, 1289. Doi.org/10.1038/s41467-020-
898 15049-7.

Always consult and cite the final, published document. See http:/www.minsocam.org or GeoscienceWorld

This is the peer-reviewed, final accepted version for American Mineralogist, published by the Mineralogical Society of America.
The published version is subject to change. Cite as Authors (Year) Title. American Mineralogist, in press.
DOI: https://doi.org/10.2138/am-2022-8712. http://www.minsocam.org/

Zhang, L., Zhang, A. C., and Wang, S. Z. (2021a) Thermal evolution of brachinite meteorites. The First National Planetary Conference. Suzhou, China. June 18–22, 2021.

Zhang, L., Zhang, A. C., and Wang, S. Z. (2021b) Mineralogical records of thermal evolution on the brachinite parent body. The Seventh Youth Geoscience Forum. Guiyang, China. July 9–11, 2021.

Zhou, Q., Yin, Q. Z., Shearer, C. K., Li, X. H., Li, Q. L., Liu, Y., Tang, G. Q., and Li, C. L. (2018) U-Pb and Pb-Pb apatite ages for Antarctic achondrite Graves Nunataks 06129. Meteoritics & Planetary Science, 53, 448–466.

Always consult and cite the final, published document. See http:/www.minsocam.org or GeoscienceWorld

This is the peer-reviewed, final accepted version for American Mineralogist, published by the Mineralogical Society of America.
The published version is subject to change. Cite as Authors (Year) Title. American Mineralogist, in press.
DOI: https://doi.org/10.2138/am-2022-8712. http://www.minsocam.org/

908 # Figure captions

909 **Figure 1**. BSE images and SEM-EDS mapping of fine-grained pyroxene-troilite
910 intergrowths in brachinites. (a) A typical pyroxene-troilite intergrowth in NWA 4969. (b-
911 d) maps of Ca, Fe, and S of the region shown in (a). (e) A region in NWA 10637 shows a
912 pyroxene-troilite intergrowth. Troilite in this region has been largely altered during
913 terrestrial weathering. (f) A region in NWA 11756 shows fine-grained pyroxene-troilite
914 intergrowths. Ol: olivine; Opx: orthopyroxene; Cpx: high-Ca pyroxene; Tro: troilite; Chr:
915 chromite.

916

917 **Figure 2**. BSE images of intergranular apatite in brachinites. (a-b) Relatively coarse,
918 irregularly-shaped apatite grains are rimmed with merrillite. Tiny pores are present in
919 merrillite grains. Note that pyroxene-troilite intergrowths are closely associated with the
920 apatite-merrillite assemblage. (c) Higher magnification image of the upper rectangle
921 outlined in (b) showing the pores in merrillite adjacent to the interface with apatite. Many
922 tiny chromite grains are present in the apatite grain interior. (d) Higher magnification image
923 of the other rectangle outlined in (b) showing the chromite grains at the boundary between
924 apatite and olivine. (e-f) Intergranular apatite and merrillite in NWA 11756. The apatite
925 grains have been partially replaced by irregular merrillite. The apatite grains contain tiny
926 acicular chromite grains. Fine-grained pyroxene-troilite intergrowths are also present

Always consult and cite the final, published document. See http:/www.minsocam.org or GeoscienceWorld

This is the peer-reviewed, final accepted version for American Mineralogist, published by the Mineralogical Society of America.
The published version is subject to change. Cite as Authors (Year) Title. American Mineralogist, in press.
DOI: https://doi.org/10.2138/am-2022-8712. http://www.minsocam.org/

adjacent to the intergranular apatite (e). Ol: olivine; Ap: apatite; Mer: merrillite; Chr: chromite; Cpx: high-Ca pyroxene; Opx: orthopyroxene; Tro: troilite.

Figure 3. BSE image (a) and SEM-EDS mapping (b-f) of apatite inclusions within an intergranular chromite grain in NWA 4969. (a) The central part of this image shows at least three grains with a Z-contrast variation in the BSE image of apatite inclusions in chromite. (c) The Cl map shows that the dark regions in (a) are relatively Cl-poor. (d) The F-rich apatite grains are indicated by yellow arrows. However, the two hot spots and the region surrounding the F-poor apatite grains in (d) show the signals from Fe $L\alpha$ rather than F $K\alpha$. (e-f) Results from Cr and S mapping. Chr: chromite; Ap: apatite; Tro: troilite.

Figure 4. BSE images of apatite inclusions in NWA 11756 and NWA 10637. (a) A euhedral apatite grain is included in an olivine grain, which itself is included in chromite from NWA 11756. (b) A rounded apatite inclusion within olivine from NWA 11756. Several euhedral merrillite grains occur at the margin of the apaite inclusion. Tiny chromite grains are also present at the boundary between the apatite and olivine. (c-d) Subhedral-euhedral merrillite grains are included in the rounded apatite inclusions within olivine from NWA 10637. Note that many tiny chromite grains occur at the boundary between apatite and olivine. Ap: apatite; Mer: merrillite; Chr: chromite; Ol: olivine; Tro: troilite.

Always consult and cite the final, published document. See http:/www.minsocam.org or GeoscienceWorld

This is the peer-reviewed, final accepted version for American Mineralogist, published by the Mineralogical Society of America.
The published version is subject to change. Cite as Authors (Year) Title. American Mineralogist, in press.
DOI: https://doi.org/10.2138/am-2022-8712. http://www.minsocam.org/

946

947 **Figure 5**. Quadrilateral diagrams showing the major-element compositions for
948 intergranular pyroxenes (a) and pyroxenes in pyroxene-troilite intergrowths (b) from the
949 brachinites in this study. InterPx: intergranular pyroxene; PTIPx: pyroxene in pyroxene-
950 troilite intergrowth. The gray regions show the compositional ranges of pyroxenes reported
951 in literature (Nehru et al., 1983; Warren et al., 1989; Swindle et al., 1998; Mittlefehldt et
952 al., 2003; Goodrich et al., 2006; Rumble et al., 2008; Goodrich et al., 2011; Gardner-Vandy
953 et al., 2013; Day et al., 2015, 2019; Crossley et al., 2020).

954

955 **Figure 6**. Al_2O_3 (a), TiO_2 (b), and Cr_2O_3 (c) vs. the Mg/(Mg+Fe) molar ratio in high-Ca
956 pyroxene from the brachinites in this study. The high-Ca pyroxene in the pyroxene-troilite
957 intergrowths shows systematically lower contents of Al_2O_3, TiO_2, and Cr_2O_3 than the
958 intergranular high-Ca pyroxene in the same meteorites, respectively. InterCpx:
959 intergranular high-Ca pyroxene; PTICpx: high-Ca pyroxene in the pyroxene-troilite
960 intergrowth.

961

962 **Figure 7**. Al_2O_3 (a), TiO_2 (b), and Cr_2O_3 (c) vs. the Mg/(Mg+Fe) molar ration in
963 orthopyroxene from the brachinites in this study. The orthopyroxene in the pyroxene-
964 troilite intergrowths shows systematically lower contents of Al_2O_3, TiO_2, and Cr_2O_3 than

Always consult and cite the final, published document. See http:/www.minsocam.org or GeoscienceWorld

This is the peer-reviewed, final accepted version for American Mineralogist, published by the Mineralogical Society of America.
The published version is subject to change. Cite as Authors (Year) Title. American Mineralogist, in press.
DOI: https://doi.org/10.2138/am-2022-8712. http://www.minsocam.org/

965 the intergranular orthopyroxene (if present) in the same meteorites. PTIOpx:
966 orthopyroxene in pyroxene-troilite intergrowth; InterOpx: intergranular orthopyroxene.

967

968 **Figure 8**. Ternary plot of apatite halogen compositions in NWA 4969 (a), NWA 10637 (b),
969 and NWA 11756 (c), compared with apatite from GRA 06128/9 (McCubbin and Jones,
970 2015). The amounts of the missing component are assumed to be 1–F–Cl. InterAp:
971 intergranular apatite; IncAp: apatite inclusion within chromite or silicate minerals.

972

973 **Figure 9**. Chondrite-normalized REE patterns of intergranular Ca-phosphate minerals in
974 in NWA 4969 (a) and NWA 11756 (b). The shaded regions show the REE patterns of
975 apatite and merrillite from GRA 06128/9 (Shearer et al., 2010; Day et al., 2012; Zhou et al.
976 2018). The reference data for the CI chondrite is adopted from Barrat et al. (2012). The
977 error bar is 1σ.

978

979 **Figure 10**. U-Th compositions of apatite in brachinites and comparison with those in other
980 extraterrestrial materials. The composition data of brachinites are from this study. The
981 composition data for apatite in GRA 06128/9 are from Zhou et al. (2018). Other
982 composition data and regions are from Ward et al. (2017) and references therein.

Always consult and cite the final, published document. See http:/www.minsocam.org or GeoscienceWorld

This is the peer-reviewed, final accepted version for American Mineralogist, published by the Mineralogical Society of America.
The published version is subject to change. Cite as Authors (Year) Title. American Mineralogist, in press.
DOI: https://doi.org/10.2138/am-2022-8712. http://www.minsocam.org/

983 Table 1. Modal abundances of minerals in three brachinites

	NWA 4969	NWA 10637	NWA 11756
Olivine	94.1	73.2	72.0
High-Ca pyroxene	2.4	3.9	6.6
Orthopyroxene	None	16.8	13.2
Plagioclase	None	0.2	0.1
Chromite	1.0	0.6	0.7
Ca-phosphates	0.1	Trace	0.1
Troilite	0.9	0.1	1.0
Fe-oxide/hydroxide	1.5	5.2	6.3
Total	100	100	100

984

985

Always consult and cite the final, published document. See http:/www.minsocam.org or GeoscienceWorld

Figure 1

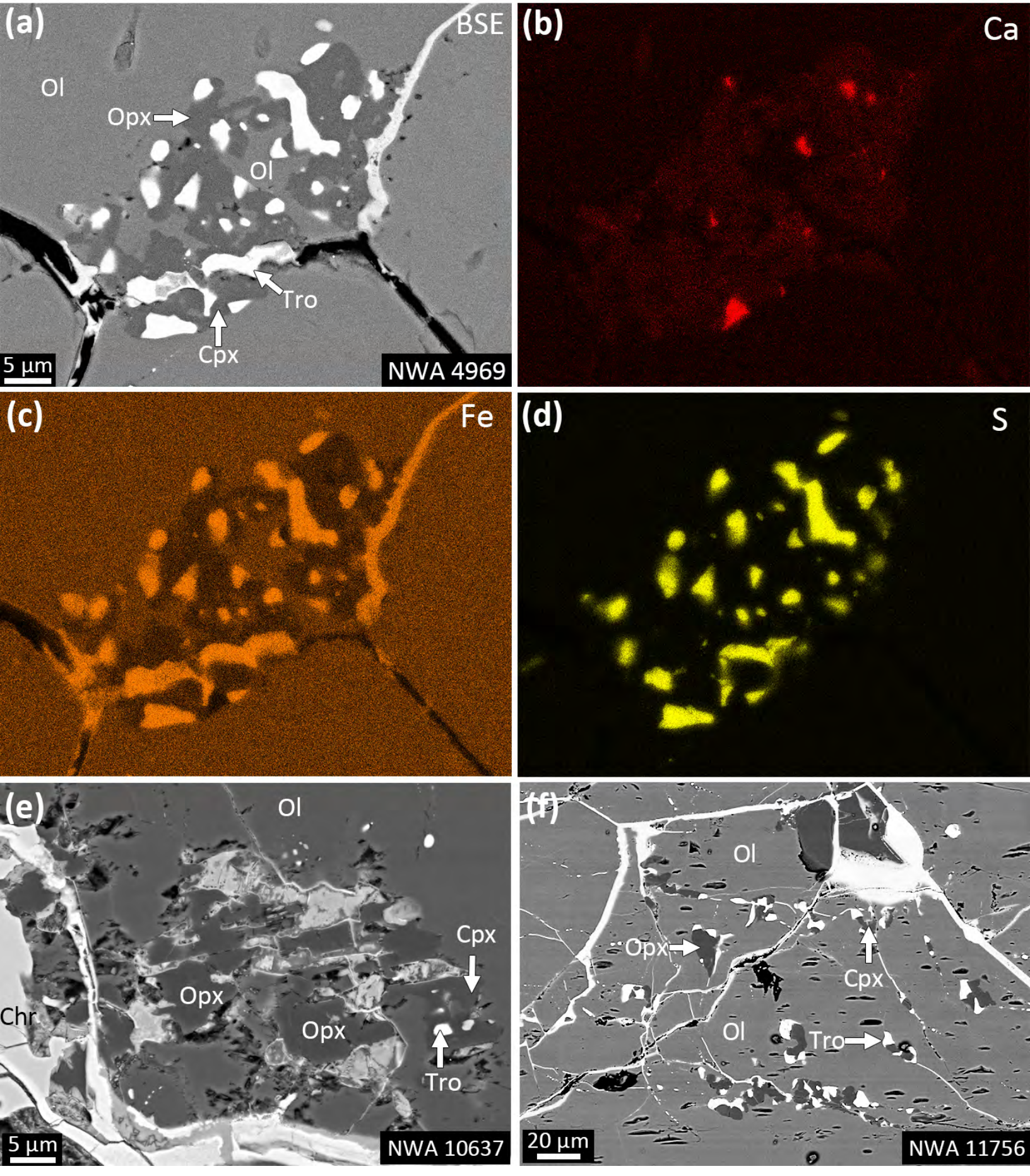
(a)
BSE
Ol
Opx
Ol
Tro
Cpx
5 µm
NWA 4969
(b)
Ca
(c)
Fe
(d)
S
(e)
Ol
Cpx
Opx
Chr
Opx
Tro
5 µm
NWA 10637
(f)
Ol
Opx
Cpx
Ol
Tro
20 µm
NWA 11756

Figure 2

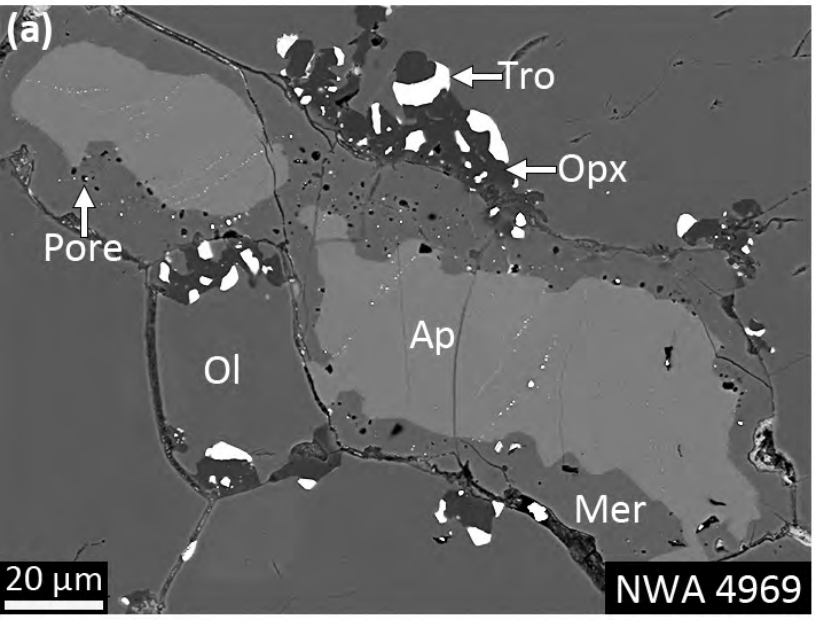
(a)
Tro
Opx
Pore
Ap
Ol
Mer
20 µm
NWA 4969

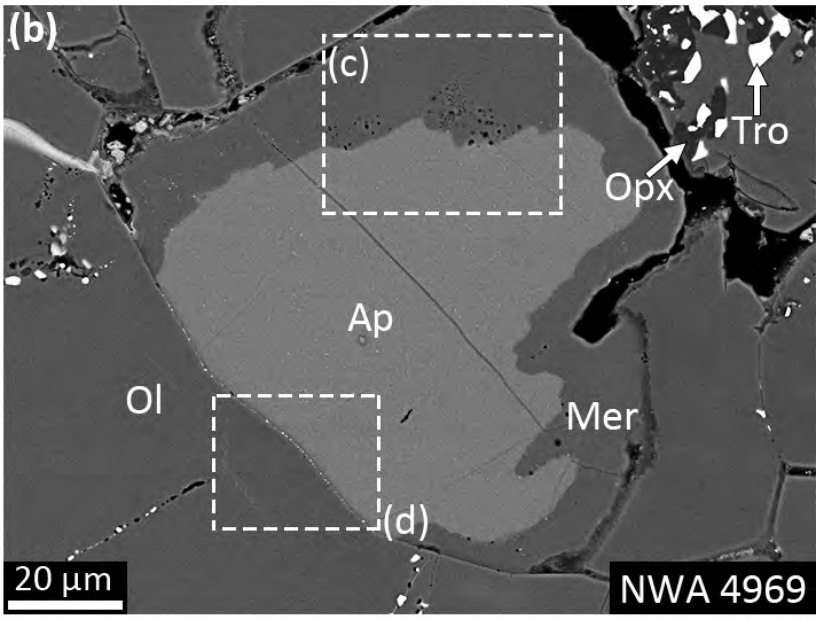
(b)
(c)
Tro
Opx
Ap
Ol
Mer
(d)
20 µm
NWA 4969

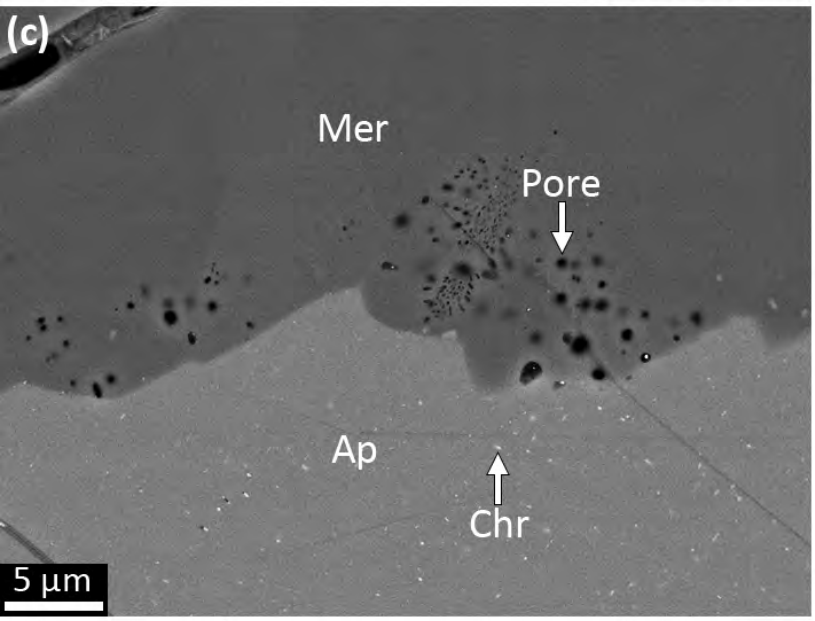
(c)
Mer
Pore
Ap
Chr
5 µm

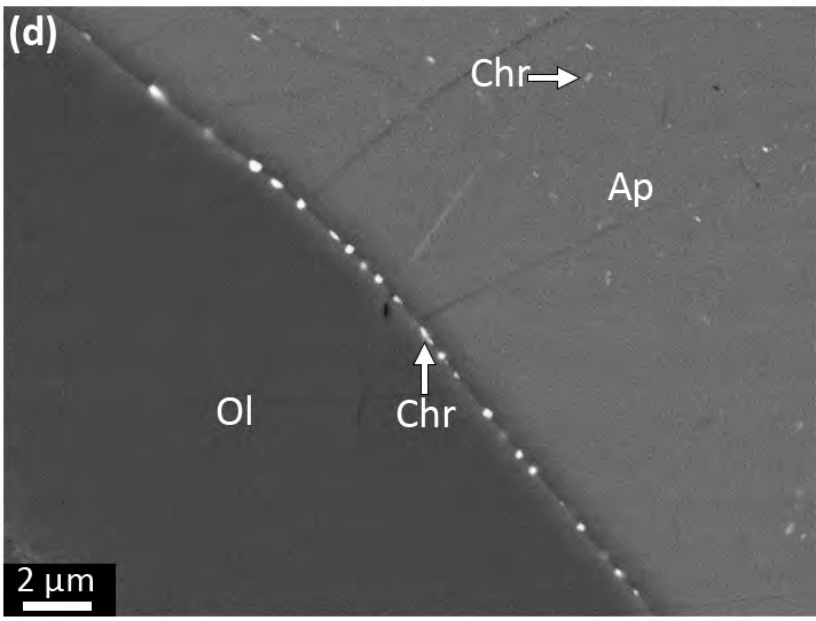
(d)
Chr
Ap
Ol
Chr
2 µm

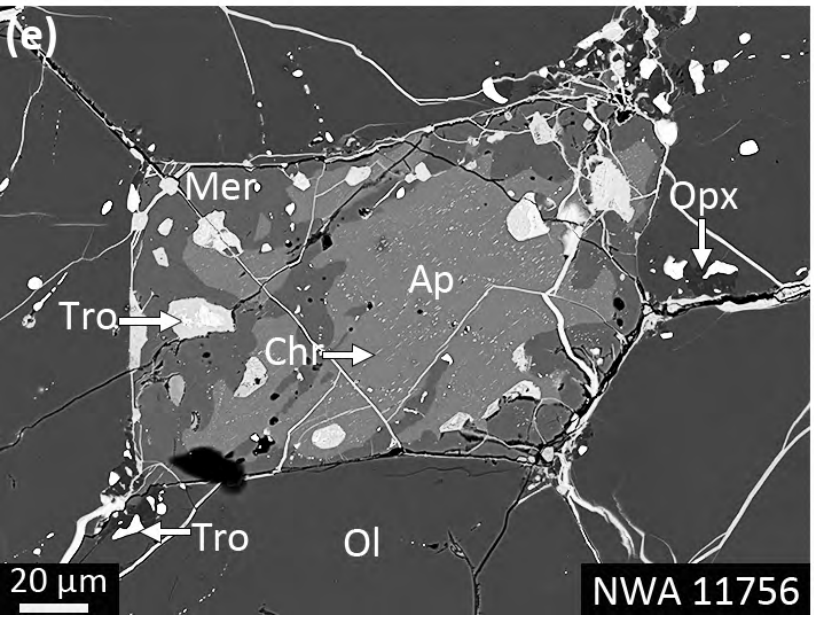
(e)
Mer
Opx
Ap
Tro
Chr
Tro
Ol
20 µm
NWA 11756

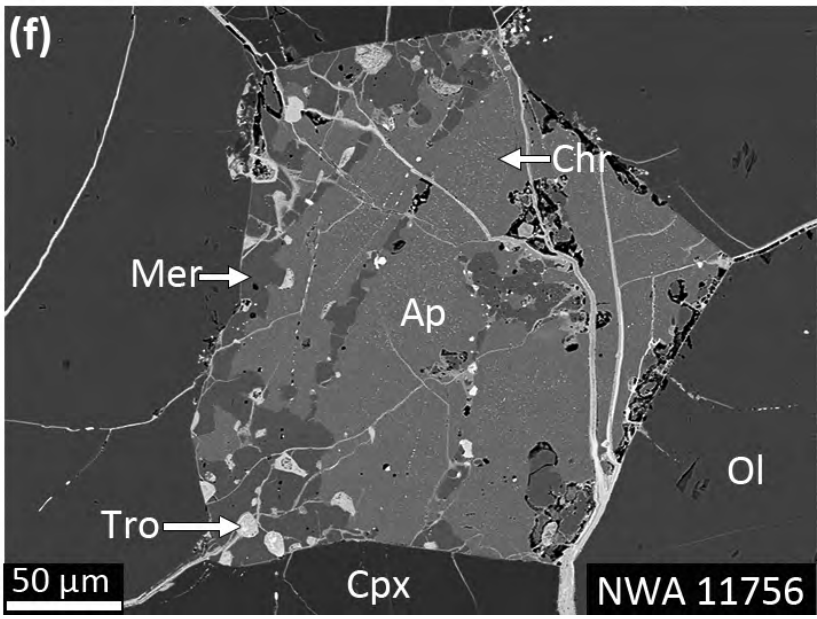
(f)
Chr
Mer
Ap
Ol
Tro
Cpx
50 µm
NWA 11756

Figure 3

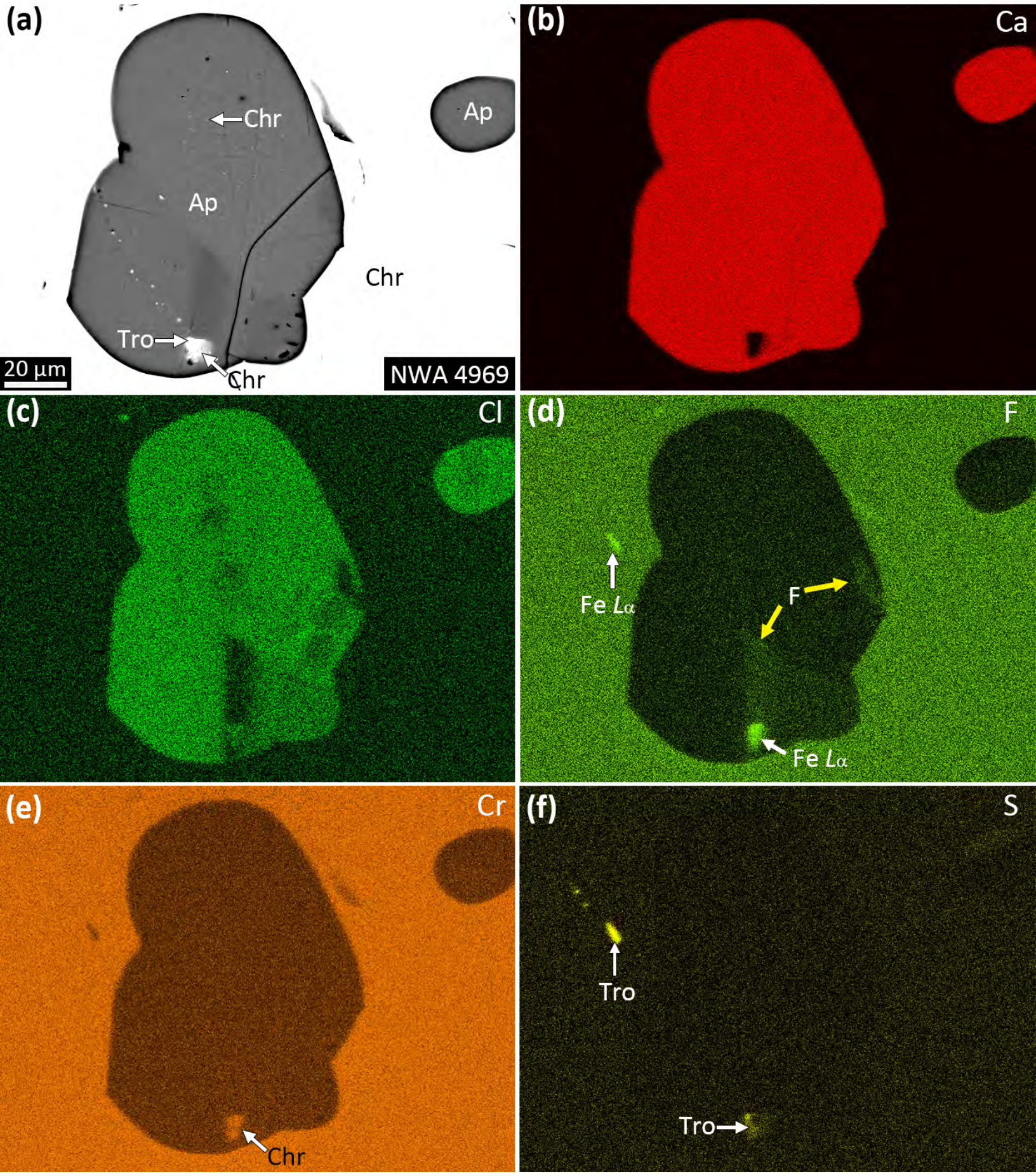
(a)
Chr
Ap
Ap
Chr
Tro
Chr
20 µm
NWA 4969
(b)
Ca
(c)
Cl
(d)
F
Fe Lα
F
Fe Lα
(e)
Cr
Chr
(f)
S
Tro
Tro

Figure 4

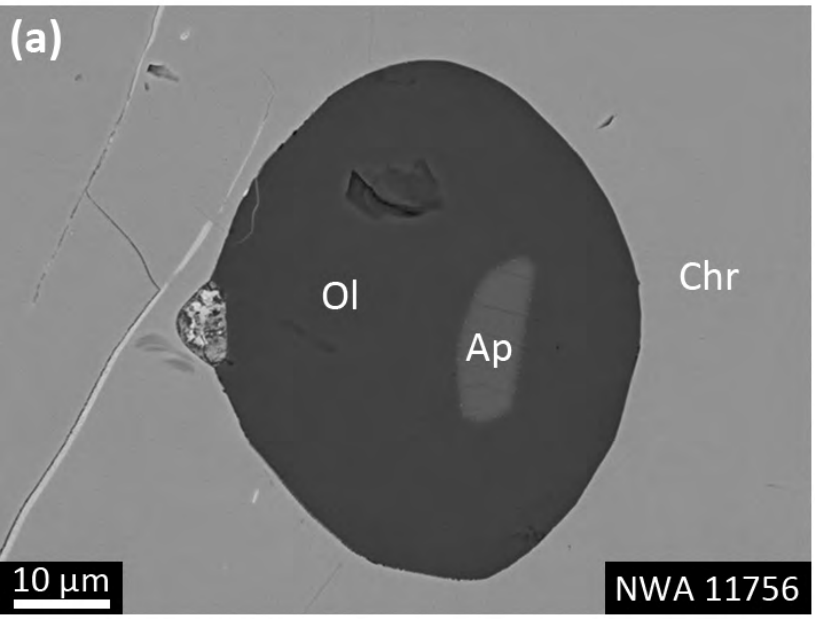
(a)
Ol
Ap
Chr
10 µm
NWA 11756

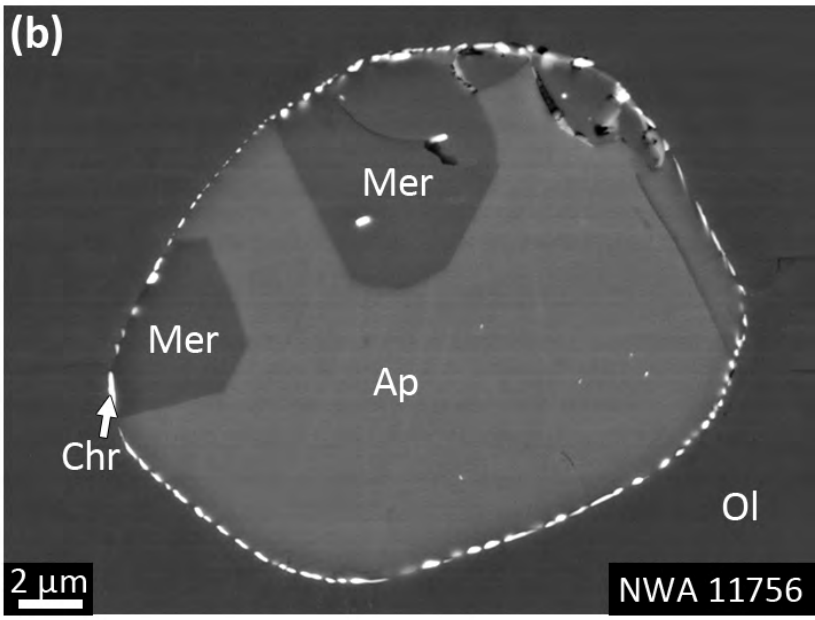
(b)
Mer
Mer
Ap
Chr
Ol
2 µm
NWA 11756

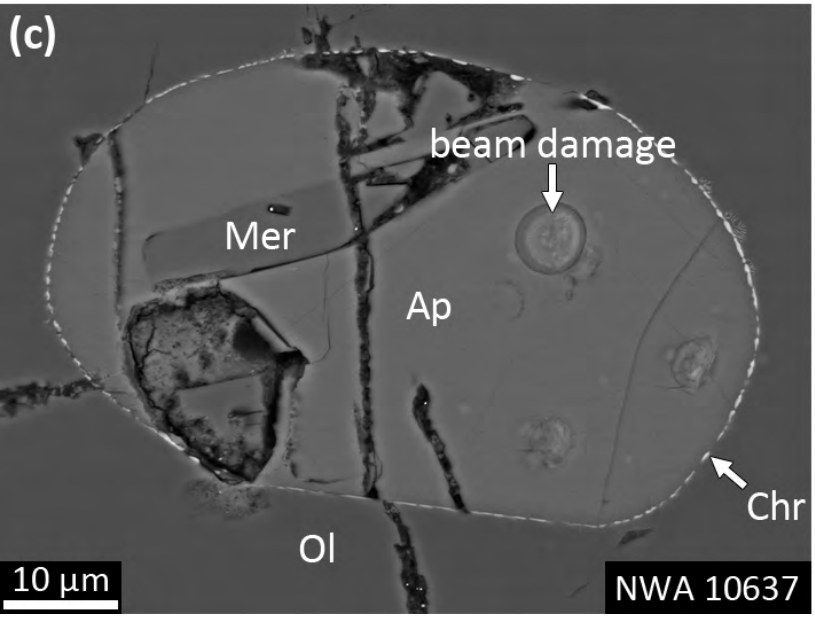
(c)
beam damage
Mer
Ap
Chr
Ol
10 µm
NWA 10637

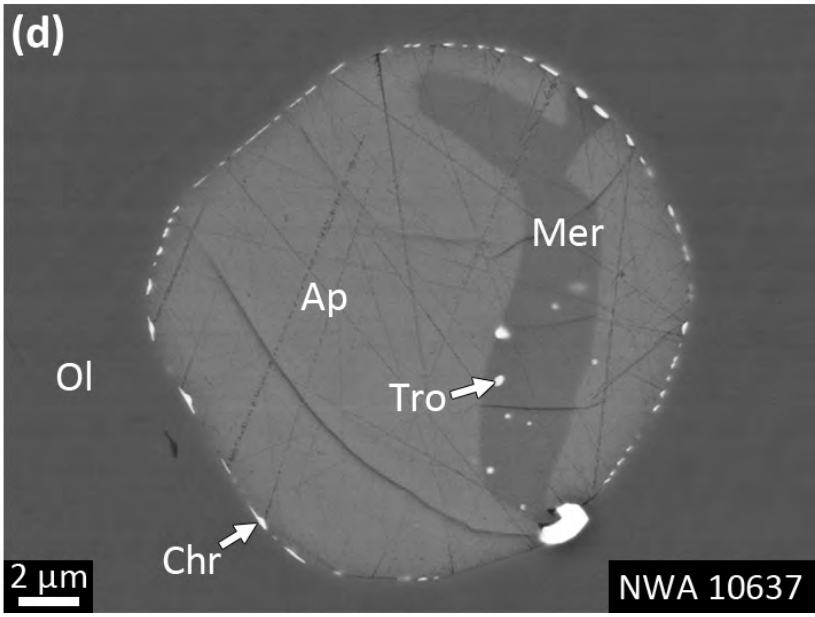
(d)
Mer
Ap
Ol
Tro
Chr
2 µm
NWA 10637

Figure 5

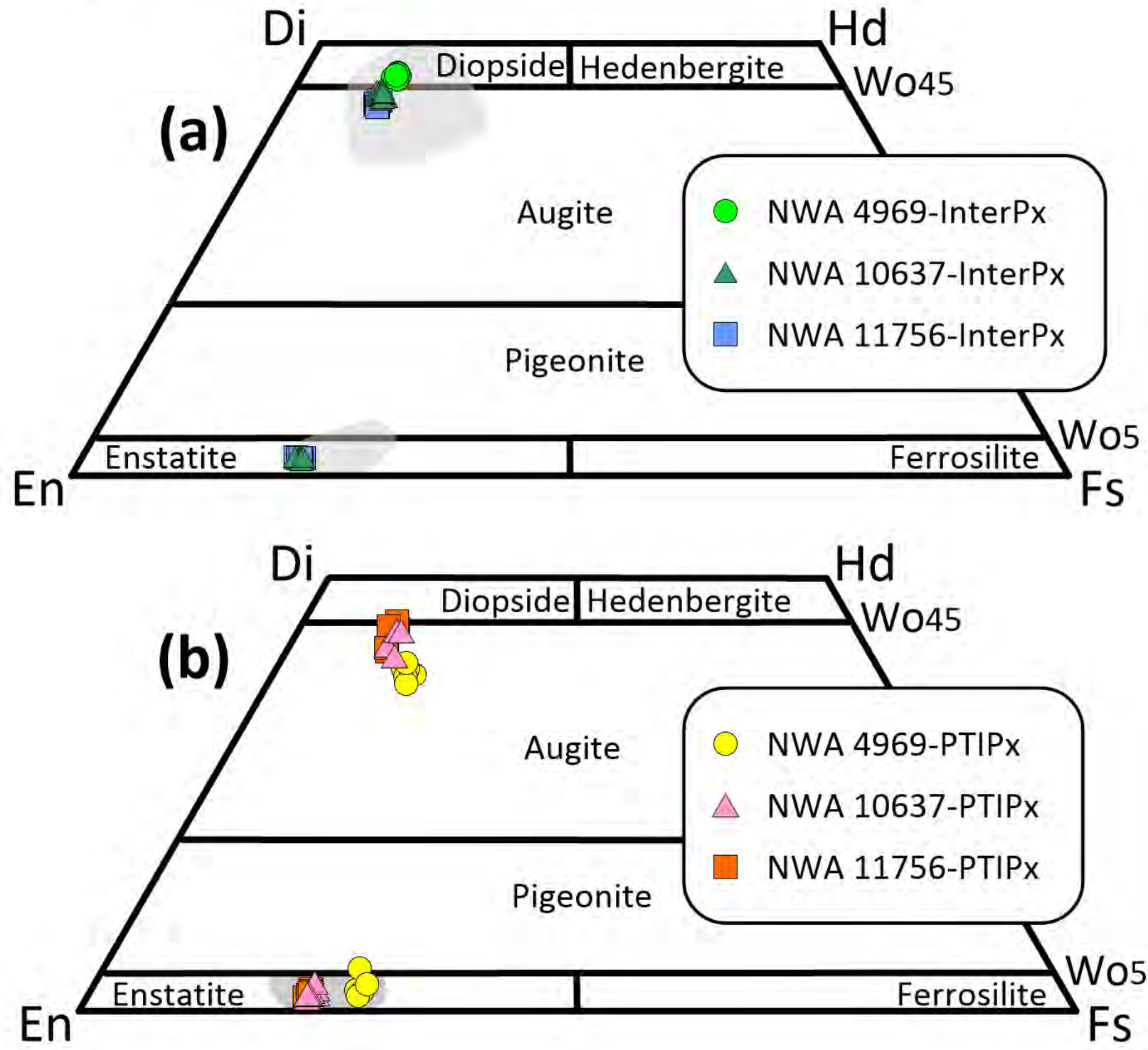
Di
Hd
Diopside
Hedenbergite
Wo45
(a)
Augite
NWA 4969-InterPx
NWA 10637-InterPx
NWA 11756-InterPx
Pigeonite
Wo5
Enstatite
Ferrosilite
En
Fs
Di
Hd
Diopside
Hedenbergite
Wo45
(b)
Augite
NWA 4969-PTIPx
NWA 10637-PTIPx
NWA 11756-PTIPx
Pigeonite
Wo5
Enstatite
Ferrosilite
En
Fs

Figure 6

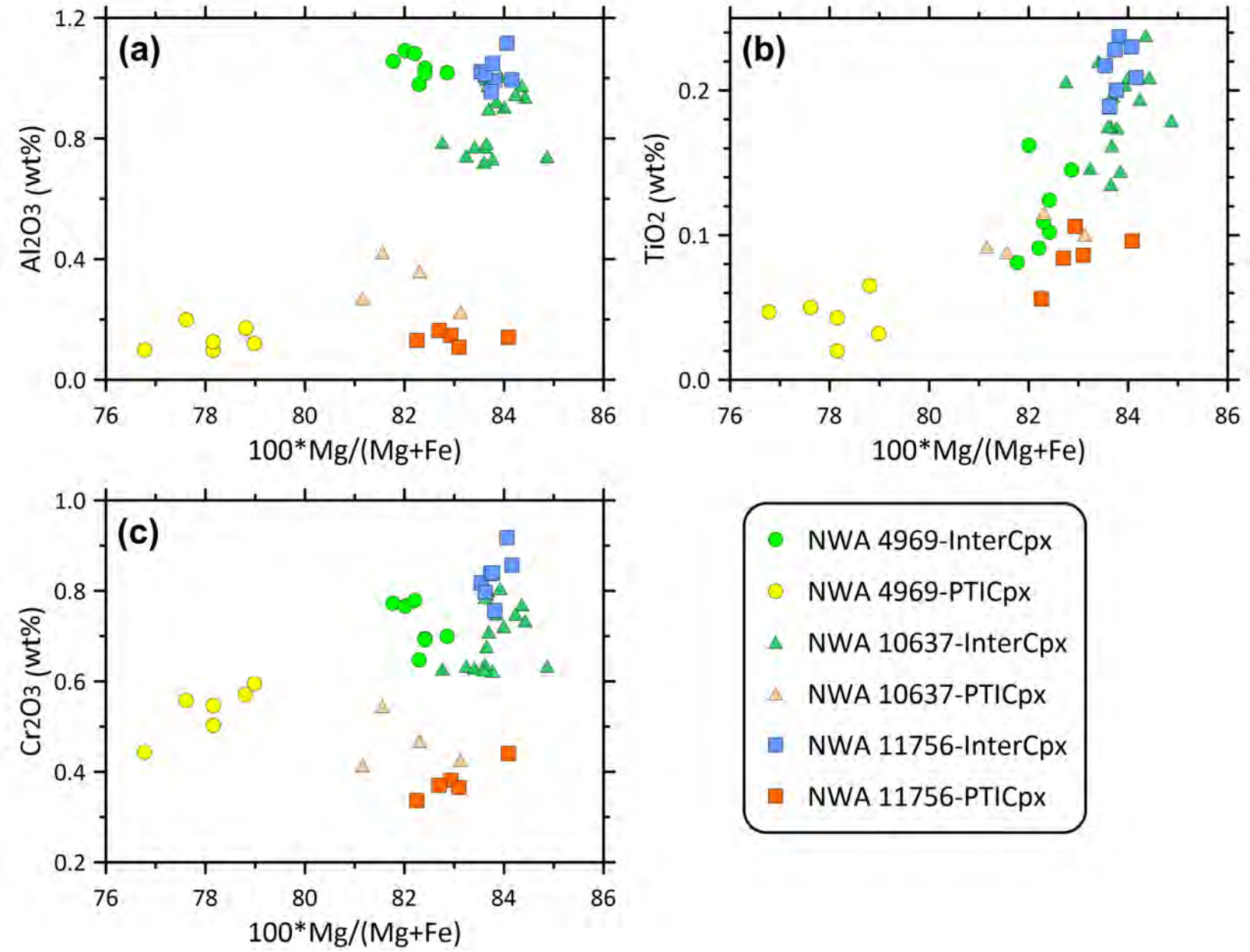
(a)
Al2O3 (wt%)
100*Mg/(Mg+Fe)
(b)
TiO2 (wt%)
100*Mg/(Mg+Fe)
(c)
Cr2O3 (wt%)
100*Mg/(Mg+Fe)
NWA 4969-InterCpx
NWA 4969-PTICpx
NWA 10637-InterCpx
NWA 10637-PTICpx
NWA 11756-InterCpx
NWA 11756-PTICpx

Figure 7

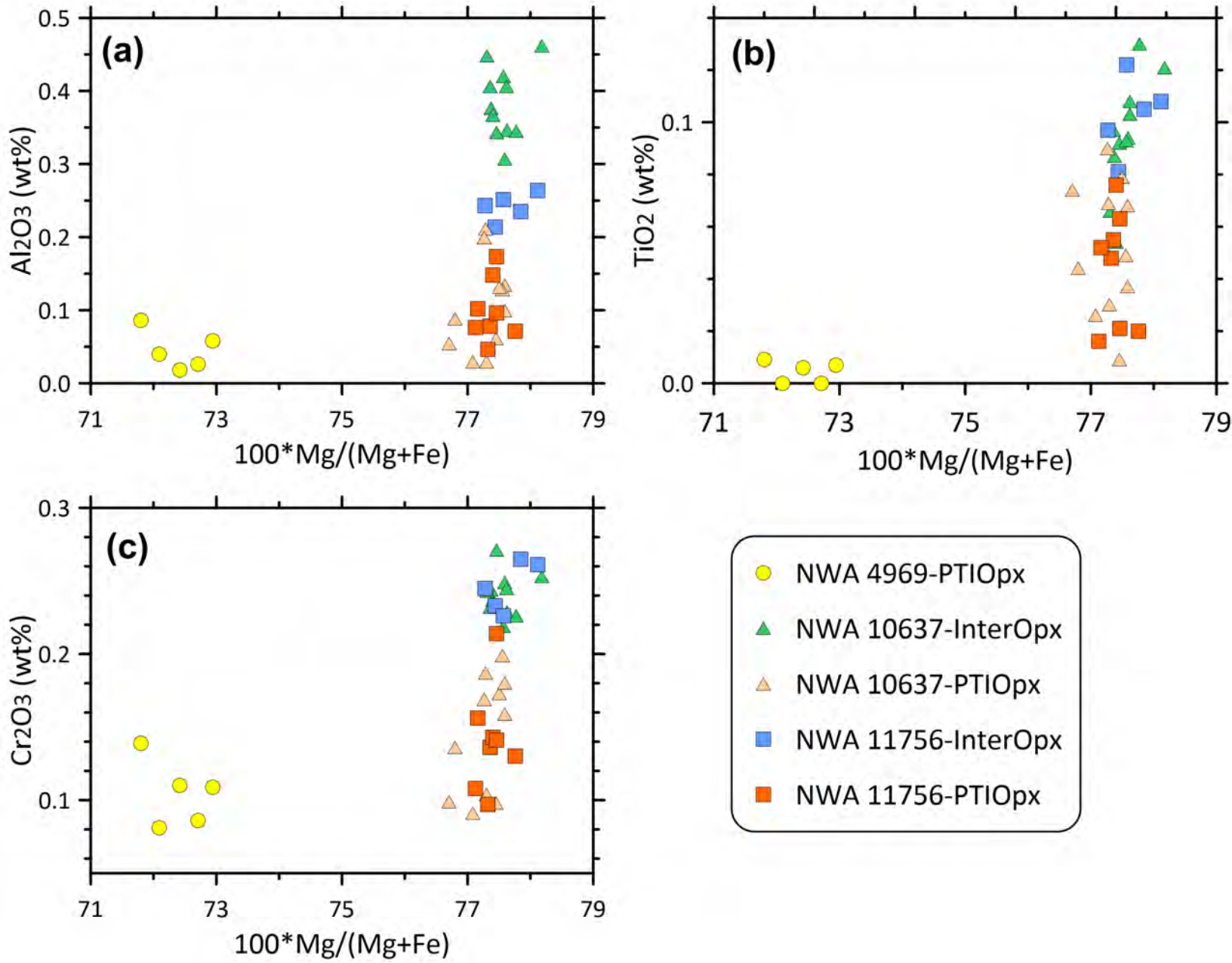
(a)
Al2O3 (wt%)
0.0
0.1
0.2
0.3
0.4
0.5
71
73
75
77
79
100*Mg/(Mg+Fe)
(b)
TiO2 (wt%)
0.0
0.1
71
73
75
77
79
100*Mg/(Mg+Fe)
(c)
Cr2O3 (wt%)
0.1
0.2
0.3
71
73
75
77
79
100*Mg/(Mg+Fe)
NWA 4969-PTIOpx
NWA 10637-InterOpx
NWA 10637-PTIOpx
NWA 11756-InterOpx
NWA 11756-PTIOpx

Figure 8

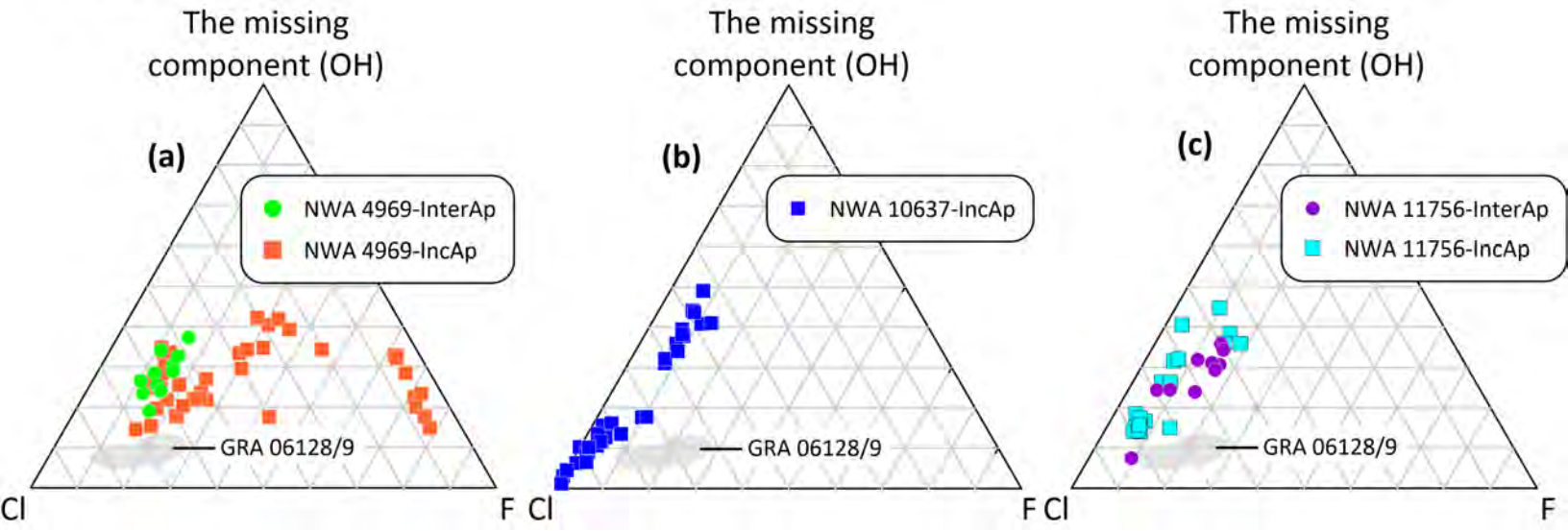
The missing component (OH)
(a)
NWA 4969-InterAp
NWA 4969-IncAp
GRA 06128/9
Cl
F
The missing component (OH)
(b)
NWA 10637-IncAp
GRA 06128/9
Cl
F
The missing component (OH)
(c)
NWA 11756-InterAp
NWA 11756-IncAp
GRA 06128/9
Cl
F

Figure 9

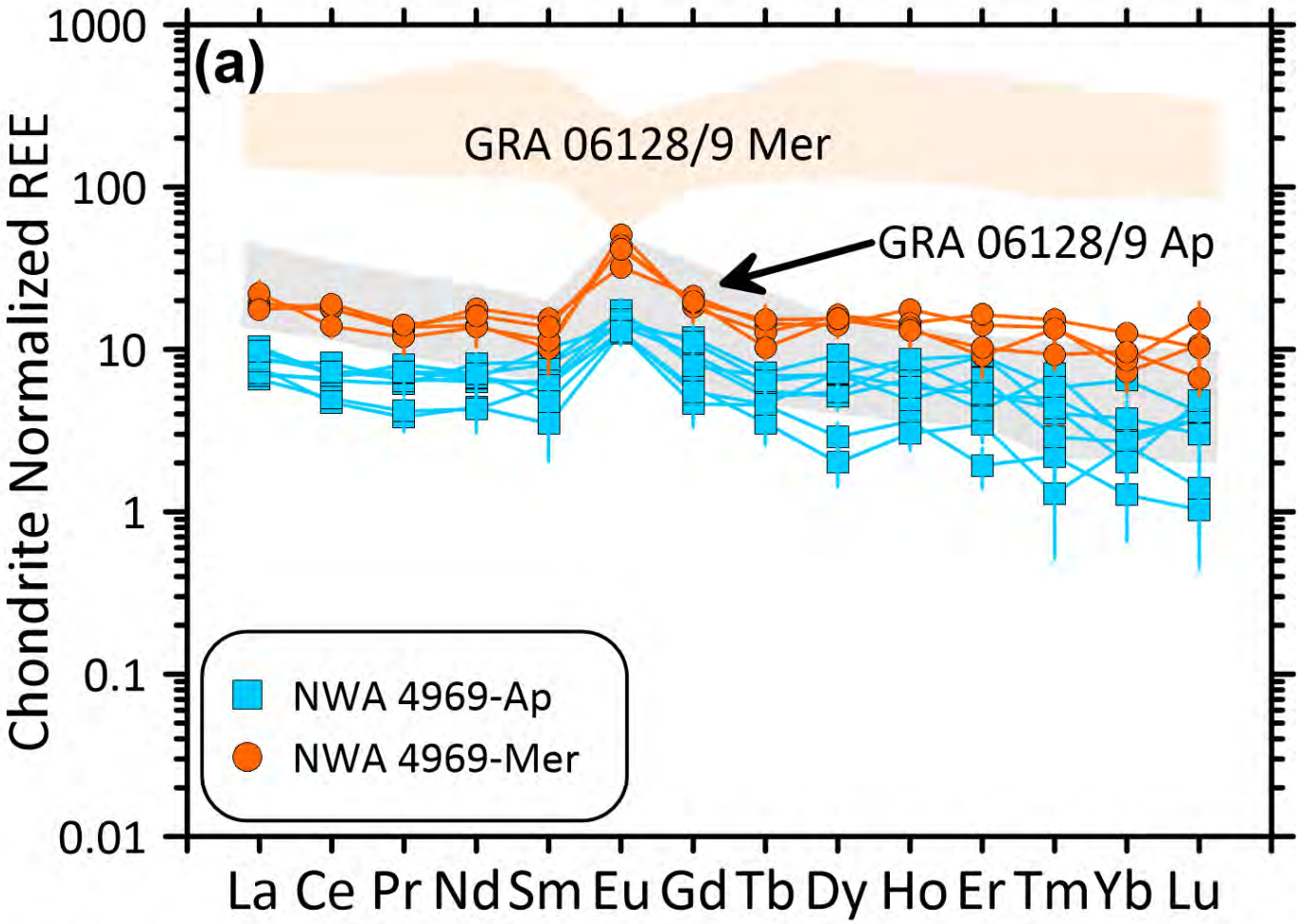
(a)
GRA 06128/9 Mer
GRA 06128/9 Ap
NWA 4969-Ap
NWA 4969-Mer
Chondrite Normalized REE
1000
100
10
1
0.1
0.01
La Ce Pr Nd Sm Eu Gd Tb Dy Ho Er Tm Yb Lu

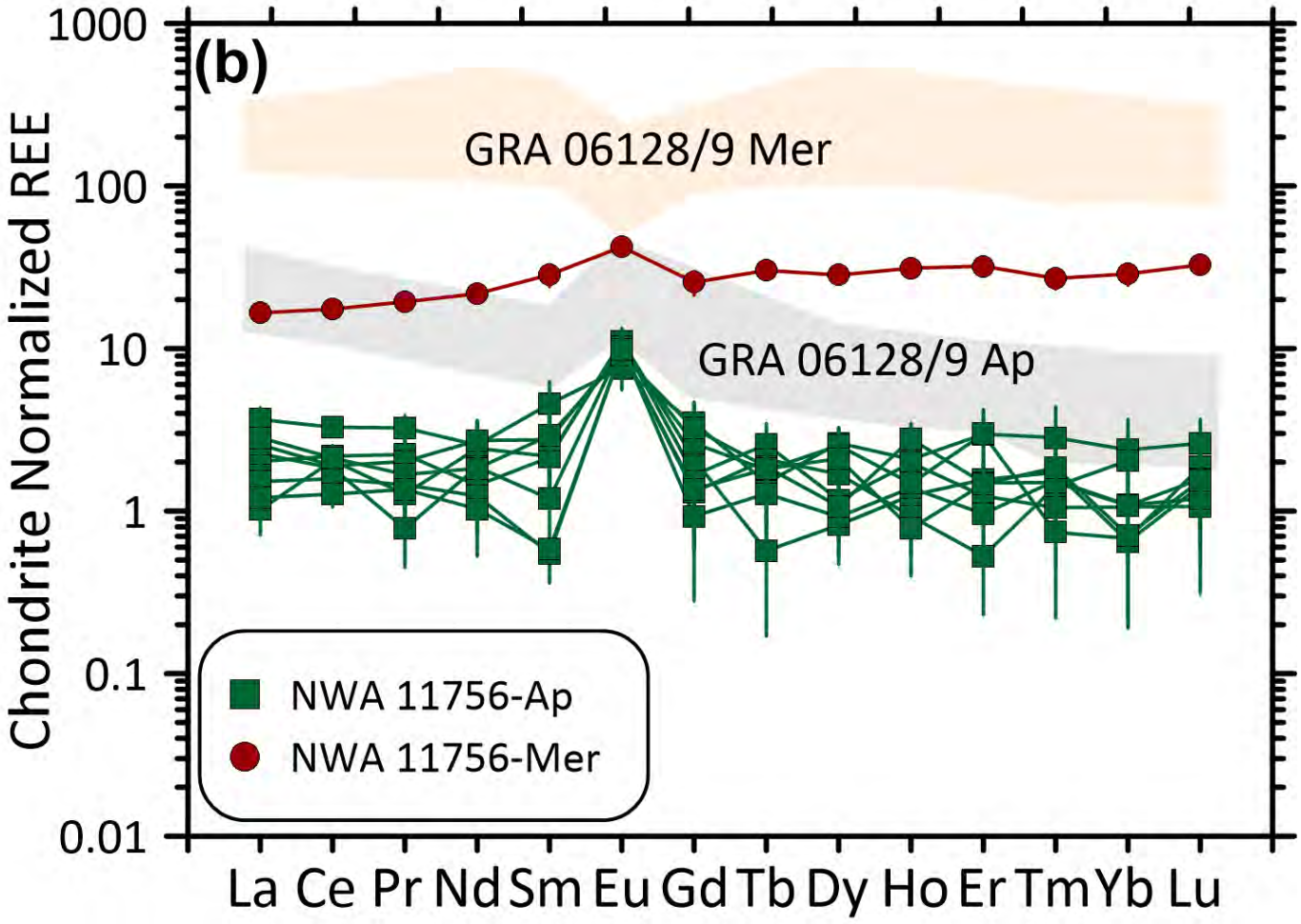
(b)
GRA 06128/9 Mer
GRA 06128/9 Ap
NWA 11756-Ap
NWA 11756-Mer
Chondrite Normalized REE
1000
100
10
1
0.1
0.01
La Ce Pr Nd Sm Eu Gd Tb Dy Ho Er Tm Yb Lu

Figure 10

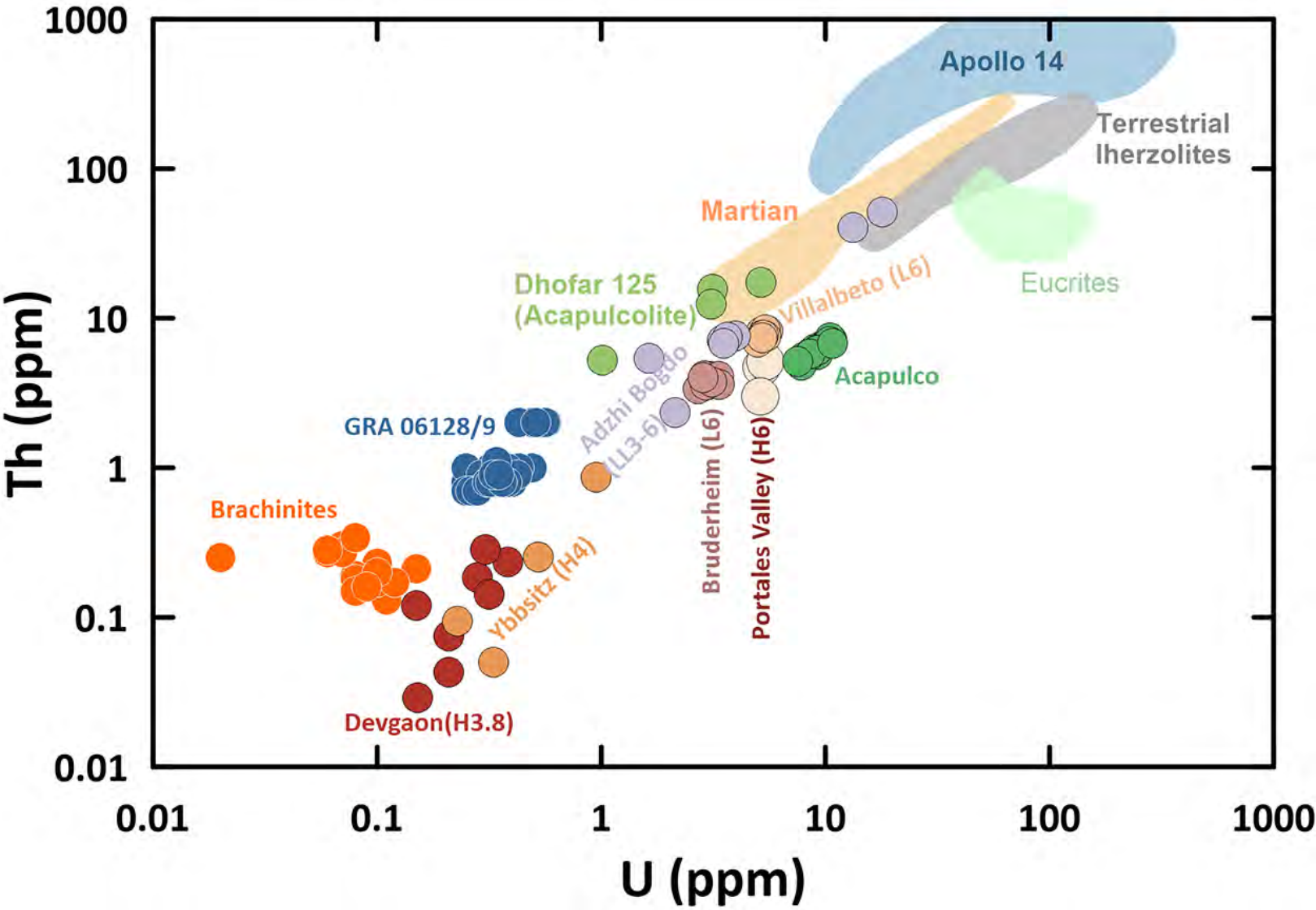
1000
100
10
1
0.1
0.01
Th (ppm)
0.01
0.1
1
10
100
1000
U (ppm)
Apollo 14
Terrestrial
lherzolites
Martian
Eucrites
Dhofar 125
(Acapulcolite)
Villalbeto (L6)
Acapulco
Adzhi Bogdo
(LL3-6)
GRA 06128/9
Brachinites
Bruderheim (L6)
Portales Valley (H6)
Ybbsitz (H4)
Devgaon(H3.8)